課題番号　　：　２４指１０３
研究課題名　：　新しい病原因子を標的とした結核ワクチンの開発
主任研究者名：　切替　照雄
分担研究者名：　切替　照雄、濱端　崇、秋山　徹、岡村　匡史、舩渡川　圭次

キーワード　：　結核菌、ワクチン、ゲノム、病原因子
研究成果　：
【目的】最近の調査で、BCG が成人結核に対して効果的でないことが明らかになった。 このように、新しいワクチンの開発は、結核の根絶のために必要である。 新しいワクチンの開発のために最も高いプライオリティーは、新しい標的分子の選抜とそのメカニズムの理解である。 この研究において、我々は、結核菌と宿主の相互作用に重要な因子を同定する。
【方法】NCGM2242 プロジェクト： 強毒結核菌 Erdman 株とその変異体株（NCGM2242）の全ゲノムを分析する。 PE_PGRS62 プロジェクト：結核菌遺伝子破壊株の相補株を作製した。結核菌 PE_PGRS62 タンパク質に結合する宿主タンパク質を同定する。Peroxiredoxin 1 プロジェクト：BALB/c バックグラウンドの Peroxiredoxin 1 欠損マウスを作製する。
【結果】NCGM2242 プロジェクト： 16s rRNA 点突然変異 U1406A（結核菌では U1399A）について記述する。この点変異は結核菌の病原性を非常に低下させるが、抗生物質のカナマイシンに抵抗性になった。 また、この弱毒株の変異は臨床分離株で観察されない変異であり、この弱毒株がワクチン株 BCG にくらべ大きなワクチン効果があることを証明した。この 16S rRNA 突然変異はリボソーム成熟に影響を及ぼすだけでなく、結核抗原 85 複合体や ESAT-6 などの病原因子、結核菌の基礎代謝に関わる酵素を含む約２０％（n = 361）のタンパク質発現を減少させた。さらにミコール酸の生合成酵素が減少したため、ミコール酸の構造が変化していた。
PE_PGRS62 プロジェクト：Δ62Comp の PE_PGRS62 タンパク質の発現回復を観察した。WT、Δ62/mock と Δ62Comp の間でどのような違いがあるかどうかを調べた。 7H9/ADC 液体培地でそれぞれの菌株の生育速度に違いがなかったが、Δ62/mock 株は J774 細胞で細胞内生存率が減少することを示した。マウスで ΔPE_PGRS62 の弱毒化するかどうかを評価するために、我々はマウスの尾静脈に、WT または ΔPE_PGRS62 を注射した。WT 感染と比較して、ΔPE_PGRS62 株感染で BALB/c と SCID マウスの生存日数が遅延した。これらの結果は、PE_PGRS62 が結核菌の病原性に必要とされることを証明した。また、新たに結核菌 PE_PGRS62 の結合タンパク質として宿主 Hornerin/S100A18 タンパク質を同定した。
Peroxiredoxin 1 プロジェクト： Peroxiredoxin 1 ノックアウトマウスは、結核菌に感受性でした。BALB/c バックグラウンドは、C57BL/6 バックグラウンドよりも結核菌への感受性が高いことが示されました。
【考察】NCGM2242 株の *rrs* 遺伝子は点突然変異し U1406A なために、NCGM2242 株の点突然変異が、復帰変異することが懸念される。更なる変異が生ワクチン開発のために必要とされる。我々は、NCGM2242 株で PE_PGRS62 遺伝子を破壊する。特に BALB/c バックグランドで、Preoxiredoxin 1 ノックアウトマウスで結核菌遺伝子破壊株の弱毒化を評価することは容易かもしれない。

Subject No. : 24S103

Title : Attenuated TB vaccine development by gene disruption of TB virulence factors

Researchers : Teruo Kirikae, Takashi Hamabata, Toru Miyoshi-Akiyama, Tadashi Okamura, Keiji Funatogawa

Key word : TB, Vaccine, Genome, virulence factor

Abstract :

【Purpose】

Recent studies have found that BCG is not effective against adult tuberculosis. Thus, the development of a new vaccine is necessary for the eradication of *tuberculosis*. The highest priority for the development of a new vaccine is the identification of a novel target molecule and the understanding of its mechanism. In this study, we will identify *M. tuberculosis* pathogenic agent, and a host factor that interacts with *M. tuberculosis* pathogenic agent.

【Method】

NCGM2242 project: A genome analysis of Erdman strain and its mutant strain (NCGM2242) were performed.

PE_PGRS62 project: A complementary strain of the *M. tuberculosis* gene knockout strain was constructed. We identified Hornerin as PE_PGRS62 binding protein. To identify the host protein(s) interacted with the mycobacterial PE_PGRS62 protein, we perform an immunoprecipitation of protein complexes followed by liquid chromatography– tandem mass spectrometry (LC-MS/MS).

Peroxiredoxin 1 project: Peroxiredoxin 1 deficient mouse with BALB/c background was constructed.

【Result】

NCGM2242 project: We describe a specific 16S rRNA mutation, U1406A (U1399A: *M. tuberculosis* number), which confers resistance to kanamycin while highly attenuating *M. tuberculosis* virulence. We also demonstrated that this attenuated strain, not observed in clinical isolates, induced greater protection against virulent *M. tuberculosis* than the *M. bovis* strain bacille Calmette-Guérin. This 16S rRNA mutation not only affected ribosome maturation but decreased the expression of ~20% (n = 361) of mycobacterial proteins, including central metabolic enzymes and virulence factors, antigen 85 complexes and ESAT-6. Furthermore, the reduced expression of mycolic acid biosynthesis enzymes resulted in alterations in mycolic acid structure.

PE_PGRS62 project: We observed the recovery of *PE_PGRS62* expression in Δ*62*Comp. We checked any difference among WT, Δ*62*/mock and Δ*62*Comp. Although we confirmed no difference among these strains grown in 7H9/ADC culture medium, Δ*62*/mock mutant showed reduced the survival of intracellular mycobacteria in J774 cells. To evaluate the virulence attenuation of Δ*PE_PGRS62* in mice, we injected WT or Δ*PE_PGRS62* into tail vein of mice. There was a significant delayed in survival with the Δ*PE_PGRS62* mutant relative to WT in BALB/c and SCID mice. These results demonstrate that *PE_PGRS62* is required for *M. tuberculosis* virulence. We identified a host Hornerin/S100A18 protein as the mycobacterial PE_PGRS62 protein binding protein.

Peroxiredoxin 1 project: Peroxiredoxin 1 deficient mouse was susceptible to *M. tuberculosis* infection. BALB/c background exhibited greater susceptibility to *M. tuberculosis* infection than C57BL/6.

【Discussion】As U1406A is mutation in *rrs* gene of NCGM2242 strain, we are concerned for revertant mutation in this strain. Further mutation is required for live vaccine development. We will disrupt *PE_PGRS62* gene in NCGM2242 strain. It might be easy to evaluate the attenuation of *M. tuberculosis* mutant in Peroxiredoxin 1 deficient mouse, especially with BALB/c background.

Researchers には、分担研究者を記載する。

24指103
研究課題名 ： 新しい病原因子を標的とした結核ワクチンの開発
主任研究者名 ： 切替　照雄
分担研究者名 ： 濱端　崇、秋山　徹、岡村　匡史、舩渡川　圭次

概要

新規の結核ワクチンを開発するためには
新たな病原因子を同定することが必須である

目　的

新たな結核菌病原因子及びこれらと相互作用する
宿主防御因子の同定

対　象

-遺伝子破壊により同定した新規病原性タンパク質
-当研究部で分離した薬剤耐性結核菌NCGM2242株

方　法

−遺伝子改変技術、マウス結核菌感染実験や結核菌ゲノム解読を実施することで対象の生物学的性状を解明する
−これらの知見をもとに結核ワクチンの候補を作製する

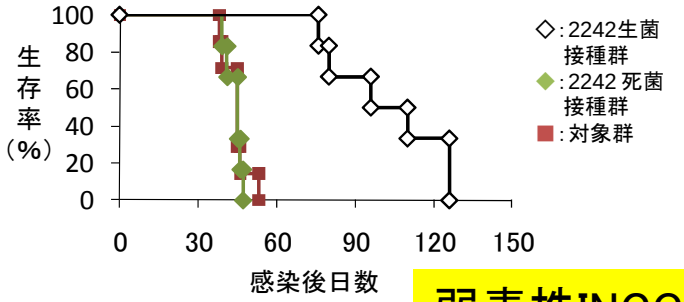

ワクチン効果

弱毒株INCGM2242

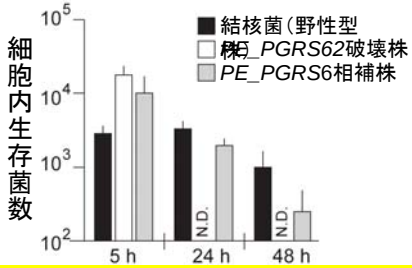

*PE_PGRS62*は病原因子

研究成果

弱毒結核菌NCGM2242株の変異の同定

結核菌弱毒株NCGM2242の全ゲノムを解読し、リボソーム点突然変異による基礎代謝酵素や病原因子のタンパク質発現が減少していることを明らかにした。

ワクチン標的分子の同定

結核菌細胞壁タンパク質のひとつであると考えられているPE_PGRS62の遺伝子を破壊し、マウス生存日数の遅延の確認により病原因子として新規に同定した。

マウス結核モデルの構築

ペルオキシレドキシン1欠損マウスは結核感受性が高かった。戻し交配によりさらに感受性を高めたBALB/cペルオキシレドキシン1欠損マウスを作製した。

結核ワクチン標的分子を選抜

NCGM2242株のリボゾーム*rrs*の点突然変異を決定し、*PE_PGRS62*を病原因子として同定した。復帰変異を防ぐためにNCGM2242株の*PE_PGRS62*を破壊する。

強毒結核菌Kurono株の全ゲノム配列解析を完了した

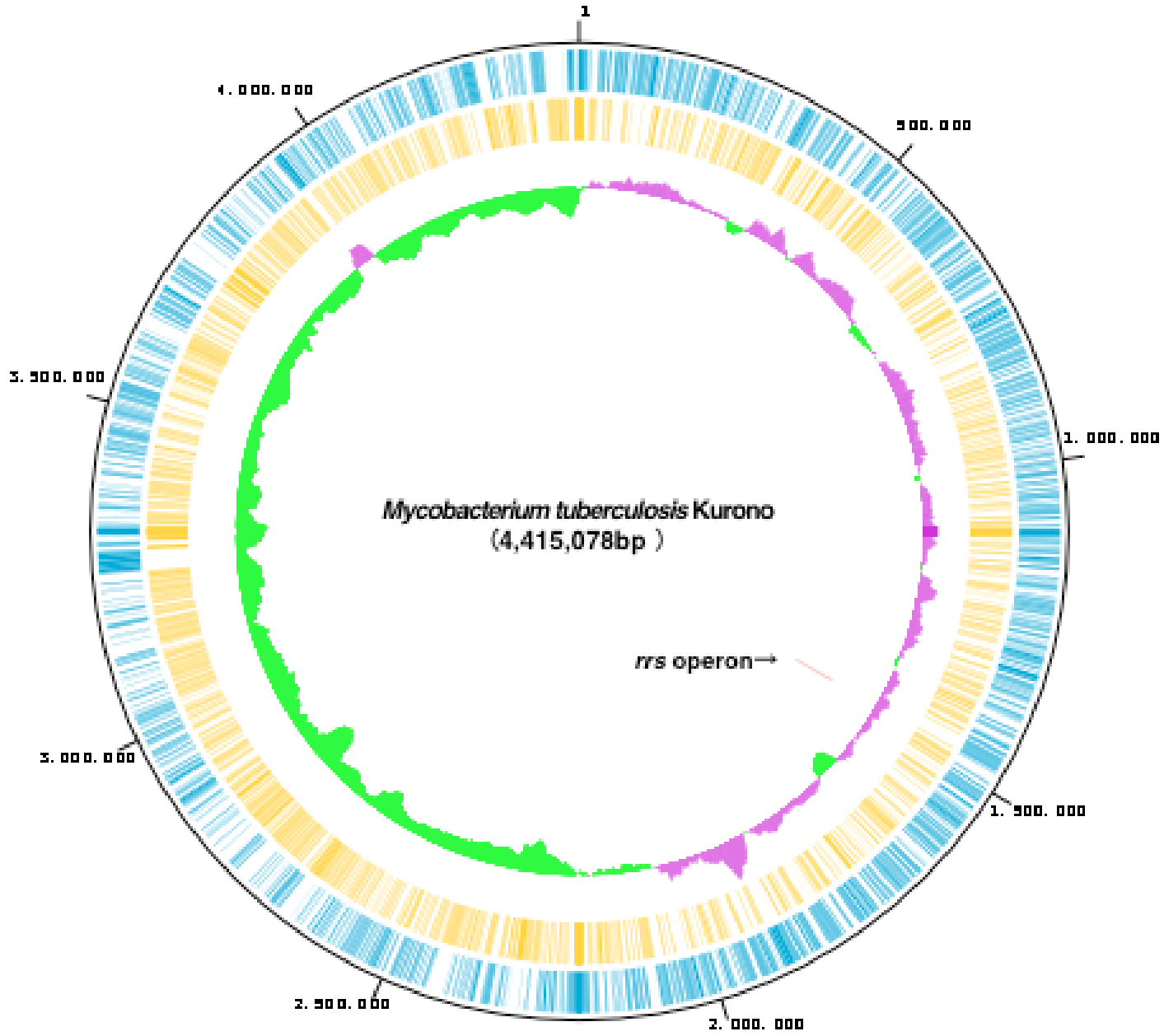

結核菌病原因子PE_PGRS62タンパク質の機能を解析した

結核菌*PE_PGRS62*を病原因子として同定した

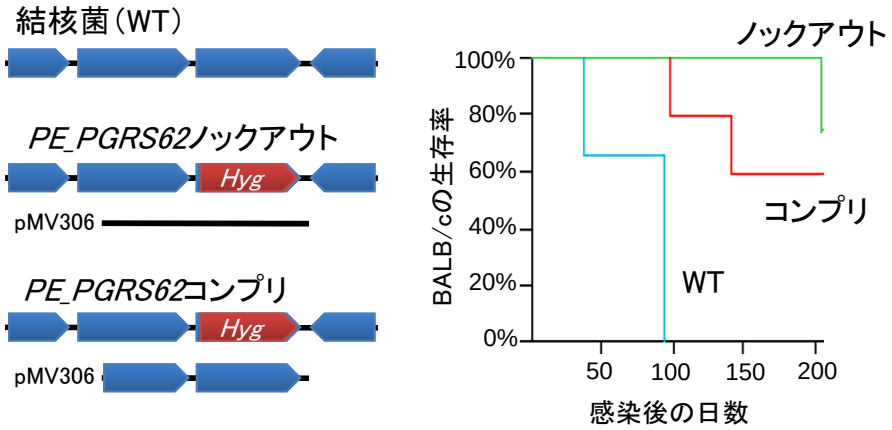

PE_PGRS62はHrnrと特異的に結合した

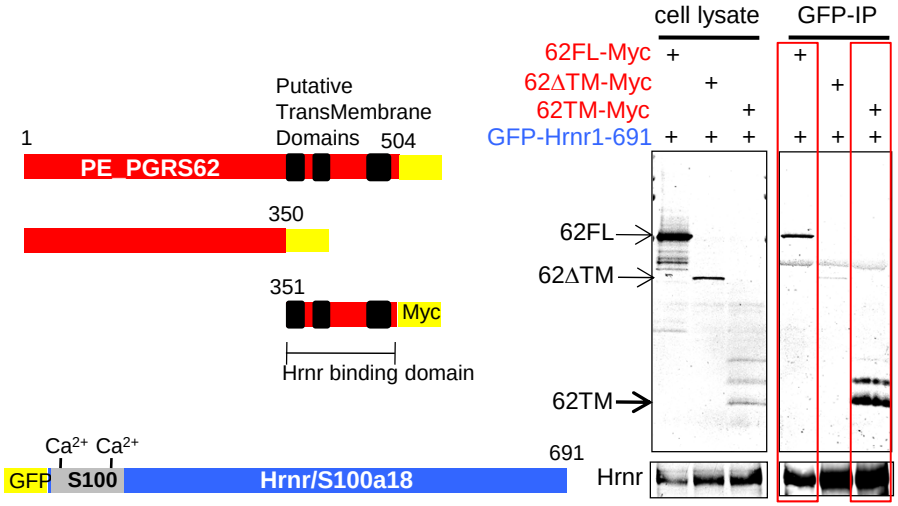

PE_PGRS62に結合する宿主タンパク質の検索

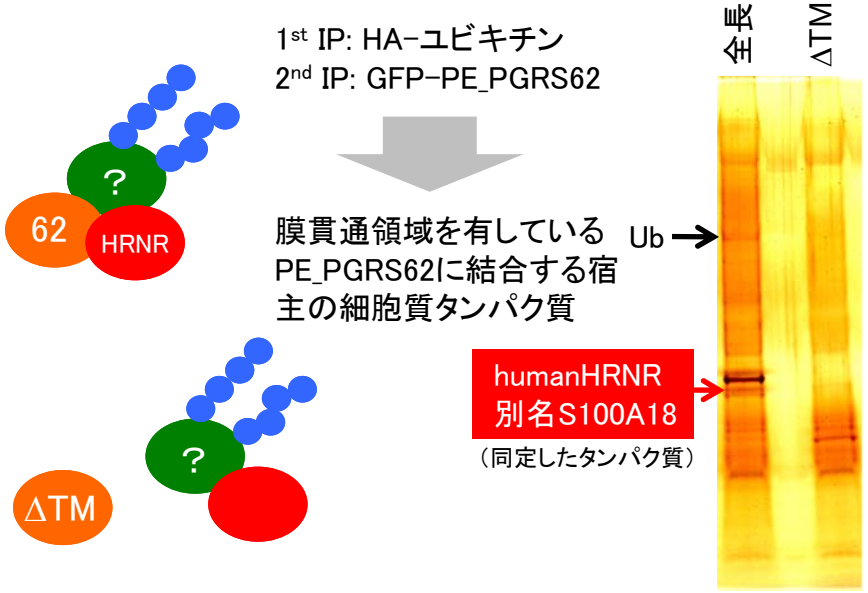

Hrnr依存的な結核菌の細胞外へのイジェクション

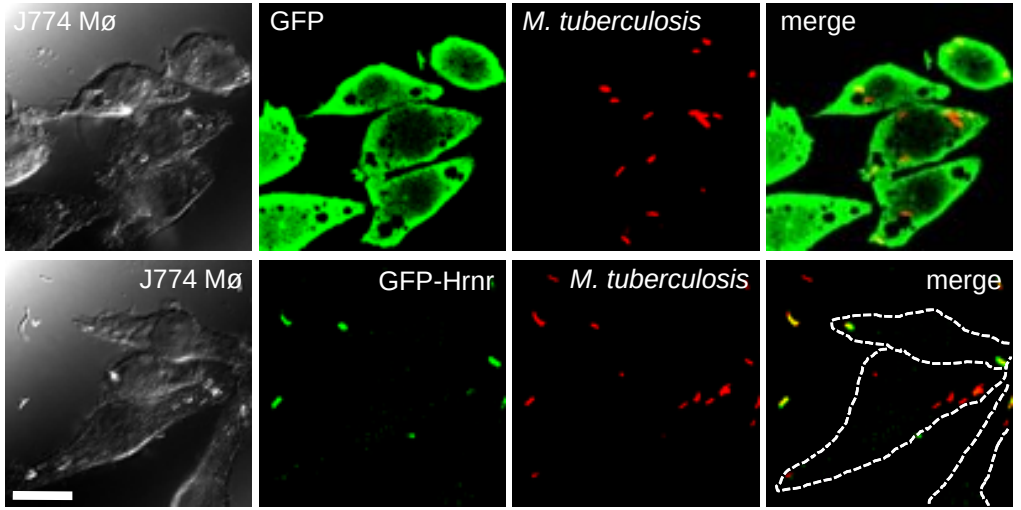

課題番号　　：24 指 103
研究課題名　：新しい病原因子を標的とした結核ワクチンの開発
主任研究者名：切替　照雄
分担研究者名：切替　照雄

キーワード　：結核菌、遺伝子破壊株、マクロファージ

研究成果　：
【目的】
BCG に代わる次世代ワクチンの開発を目指して、複数変異を導入する親株として弱毒結核菌でワクチン効果を示す NCGM2242 株を得た。全ゲノムシークエンスの結果から NCGM2242 株は *rrs* 遺伝子の点変異体であることが明らかになったが、この変異がプラスミドにより *rrs* 発現を相補することで、種々のフェノタイプ（菌の増殖性、薬剤耐性の獲得、リボソーム RNA の成熟、ワクチン効果など）が回復するかどうかを調べる必要がでてきた。相補実験の結果、NCGM2242 株が *rrs* の点変異が原因でワクチン効果があることが確認された場合は、復帰変異が起こらないように既に同定している病原因子 *PE_PGRS62* の破壊を行いワクチン候補株（NCGM2242 バックグラウンド・*PE_PGRS62* ノックアウト）の作製を目指す。
病原因子として同定した結核菌 PE_PGRS62 や PE_PGRS62 結合タンパク質である Prdx1 の機能解析を通じて、結核菌感染に重要な役割を果たす新たな宿主因子を発見する。

【方法】
rrs を相補するために *rrs* を含むオペロン領域（～8kbp）をエピソーマルなプラスミド（ゼオシン耐性）に挿入し、NCGM2242 株にエレクトロポレーションで導入、*rrs* コンプリ株を作製する。
PE_PGRS62 の結合タンパク質であった Hornerin を安定発現する J774 マクロファージを作製し、結核菌感染における Hornerin の役割を共焦点レーザー顕微鏡により解析する。

【結果】
ゼオシン耐性マーカー遺伝子を有するプラスミドを作製した（pHI191）。*rrs* オペロン 8 kbp を pHI191 に挿入し、NCGM2242 株に導入した（rrs コンプリ株）。rrs コンプリ株が、病原性復帰傾向であることを調べるために、マウスへの感染実験を実施中である。
Hornerin の発現依存的に結核菌がマクロファージ細胞外にイジェクトすることが観察された。

【考察・結論】
NCGM2242 の全ゲノムシーケンスにより rrs 変異が明らかとなりリボソーム変異により低代謝なことがわかった。しかしながら、rrs 以外の変異の可能性がないかどうかを示すために、rrs コンプリ株の作製および病原性復帰や表現型解析が必要になった。rrs コンプリ株が完成したので、NCGM2242 株の弱毒化が rrs の変異だけであることが証明できそうである（実験中）。
同定した宿主因子である Hornerin が結核菌感染に重要な役割を果たす可能性が示唆された。したがって、より信憑性が高い実験結果を得るために、導入済みの CRISPR/Cas9 システムを用いた迅速な Hornerin ノックアウトマウスの作製を行い、結核菌感受性を調べる必要がでてきた。現在、Hornerin ノックアウト BALB/c マウスを作製中である。

課題番号　　：24 指 103
研究課題名　：新しい病原因子を標的とした結核ワクチンの開発
主任研究者名：切替　照雄
分担研究者名：濱端　崇

キーワード　：結核菌、PE_PGRS62、Hornerin

研究成果　：
【目的】
結核は国際的な再興感染症であり、予防には BCG が用いられている。BCG は乳幼児期の重傷化する結核を予防できるが、成人の結核を予防する次世代ワクチンが開発されていない。そこでワクチンの開発を目指し、これまでに作製した弱毒株である遺伝子ノックアウト結核菌の病原性低下のメカニズムを明らかにするために、PE_PGRS62 タンパク質の宿主細胞内における機能を明らかにする。

【方法】
結核菌 PE_PGRS62 タンパク質に結合する宿主タンパク質の同定：同定した結核菌病原因子タンパク質 PE_PGRS62 の機能を明らかにするために、宿主細胞内で PE_PGRS62 を発現させ観察を行った。結合タンパク質を同定するために２段階の免疫沈降、具体的には GFP-PE_PGRS62 と HA-ユビキチンを共発現させた 293T 細胞の抽出液を用いて HA 抗体による１回目の免疫沈降後に GFP 抗体による２回目の免疫沈降を行い、得られた特異的な銀染色バンドを LC-MS/MS 解析し、PE_PGRS62 に結合する宿主タンパク質を同定する。
結核菌 PE_PGRS62 タンパク質を発現する肺胞 II 型上皮細胞 A549 の作製：A549 細胞に安定的に GFP-PE_PGRS62 を発現させるために、レトロウィルスベクター（pMX-puro、pVSV-G プラスミドと Plat-GP 細胞によるシステム、Cell biolabs 社）を使用し *GFP-PE_PGRS62* 遺伝子を含む DNA 断片を A549 細胞に導入する。ピューロマイシン耐性細胞株を限界希釈により分離し、生育後に細胞抽出液を作製し Anti-GFP 抗体でウェスタンブロッティング解析を行うことで GFP-PE_PGRS62 が安定発現した A549 細胞をクローニングする。

【結果・考察】
PE_PGRS62 タンパク質を 293T 細胞に過剰発現させるとベシクルに局在することがわかった。このベシクルに関与している細胞質タンパク質を同定するために、細胞質に豊富に存在しているユビキチンタンパク質を過剰発現・免疫沈降してから GFP-PE_PGRS62 の免疫沈降を行ったところ、結合タンパク質として Hornerin を同定した。Hornerin と PE_PGRS62 の結合が C 末端領域の推定膜貫通領域であることも確認できた。
Hornerin はケラチノサイトで発現量が多いことがわかっていた。結核菌感染に関係しそうな A549 細胞（肺胞 II 型上皮細胞株）と Jurkat 細胞（T 細胞株）で Hornerin が比較的多く発現していることがわかってきた。マクロファージの他に肺胞 II 型上皮細胞は結核菌が直接感染することが知られており、この細胞内で PE_PGRS62 タンパク質が機能する可能性が考えられたため、GFP-PE_PGRS62 を安定発現する A549 細胞を作製した（クローン No.11 細胞）。
A549 細胞内で GFP_PGRS62 はベシクルに局在することが確認され、このベシクルがラメラ封入体であるかどうかを確認するために、クローン No.11 細胞に安定的に ABCA3-Myc を発現する細胞株を作製中である。
A549 細胞はサーファクファクタントタンパク質の分泌等が不完全であることが知られている。これまでに我々の研究グループが同定した PE_PGRS62 結合タンパク質である宿主 Prdx1 は細胞質型のペルオキシレドキシンとして知られているが、A549 細胞において TGF-b1 刺激依存的に細胞外に分泌することが報告されている。Prdx は細胞内では抗酸化作用を示すと考えられているが、Prdx がマクロファージや樹状細胞を TLR2/TLR4 依存的に IL-23、IL-1b、TFN-a などの炎症性サイトカインを強く産生させることが知られている。現在、A549 細胞を用いた Prdx1 の分泌を調べる実験系を構築中である。Prdx1 の分泌を PE_PGRS62 と Hornerin がどのように制御するか明らかにすることで結核菌の新たな感染戦略を発見できる可能性が十分ある。

課題番号　　：24 指 103
研究課題名　：新しい病原因子を標的とした結核ワクチンの開発
主任研究者名：切替　照雄
分担研究者名：秋山　徹

研究成果　　：
【目的】新規の結核ワクチンを開発するためには、新たな病原因子を同定することが必須である。本研究では、新たな結核菌病原因子およびこれらと相互作用する宿主防御因子を同定するための基盤として、結核菌の全ゲノム情報を詳細に解析するために、結核菌実験株として動物実験などに汎用される Kurono 株の全ゲノム配列解析を実施した。
【方法】Kurono 株は全ゲノム配列を次世代シーケンサにより取得した。Annotation は glimmer 3.0 による CDS 抽出後、代表的な結核菌株である H37Rv 株の配列を参照しながら、in sillico molecular cloning（インシリコバイオロジー社）で自動的に予備 annotation を行った後、マニュアルで補正した。
【結果】Kurono 株の全ゲノム配列の解析を完了した。総コンティグ塩基数は 4,455,125,637bp であり、既知の結核菌のゲノムサイズのほぼ 100 倍のデータ量を得ることができた。約 50 倍 coverage の Illumina1 ショートリードによる SNP レベルのエラーの有無について確認したところ、エラーはまったく検出されなかった。Kurono 株の全ゲノム塩基数は 4,415,078bp で他の結核菌と同様 rrs オペロンは 1 個のみ存在した（図１）。蛋白質コード領域は 4340 個と推定された。tRNA 遺伝子数は 53 個、tmRNA 数は 1 個、IS6110 配列は 14 個存在した。既知の薬剤耐性に寄与する変異は認められなかった。Large sequence polymorphisms 法による系統解析では、Kurono 株は Euro-American 系統に分類された。

現在までに全ゲノム配列が完全決定された結核菌は Kurono 株を含めて 16 株である。全ゲノム配列を用いた系統解析では、Kurono 株は H37Rv と最も近縁であり、SNP レベルの変異はわずか 818 個だった。これらの SNP の約 40%は、結核菌ゲノムの中で特に変動が大きいとされている、PE-PPE ファミリ蛋白質の中に存在していた。

。
【考察・結論】これまでに他の菌種で実施したゲノム解析の経験を元に、結核菌実験株として著名である Kurono 株の全ゲノム配列解析を完了した。

課題番号　　：24指103
研究課題名　：新しい病原因子を標的とした結核ワクチンの開発
主任研究者名：切替　照雄
分担研究者名：岡村　匡史

キーワード　：マウス、結核、感受性遺伝子、連鎖解析
研究成果　　：

分担研究課題：結核ワクチン評価モデルの開発およびマウス結核感受性遺伝子の同定

［目的］

BCG ワクチンは小児の結核性髄膜炎や粟粒結核を有効に予防するものの、成人の肺結核には無効であることが大規模な疫学検査から明らかとなっている。従って、成人の肺結核に対して本当に有効なワクチンは未だ存在しない。その原因の一つとして、有用な結核感染モデル動物の開発が遅れていることが上げられる。我々は、結核の病原因子として、PE_PGRS62 を同定し、PE_PGRS62 は宿主細胞のペルオキシレドキシン(Prdx1)と特異的に結合し、Prdx1 遺伝子欠損マウスでは、結核菌に対する感受性が著しく高い事を見出した。さらに、Balb/c マウスは、C57BL/6 比べ、遺伝的に結核菌に高感受性を示す形質を有している。本研究では、以上の知見およびツールを用いて、新たな結核菌評価モデルを開発するとともに、結核菌病原因子と相互作用する宿主防御因子を同定することを目的とする。

[結果および考察]

１．結核菌高感受性マウスを用いたワクチン候補株の検証

Prdx1 遺伝子を欠損することで、マウスは結核菌に対する感受性が著しく高まる。さらに、結核菌に感受性が高い系統である BALB/c に Prdx1 欠損を導入した結核菌高感受性マウス（Prdx1$^{-/-}$-BALB/c）は、ワクチン候補株やリコンビナント病原因子のワクチン効果をより効率的に評価できるモデルとして期待される。ワクチン候補株である弱毒株 NCGM2242 を結核高感受性 Prdx1$^{-/-}$-BALB/c に接種し、そのワクチン効果を検証した。その結果、NCGM2242 を接種したことで、逆に発症が早まってしまった。NCGM2242 にワクチン効果はなかったが、Prdx1$^{-/-}$-BALB/c は、BALB/c よりも結核菌に高感受性であるため、ワクチンの安全性およびその効果の検証に有用であると考えられた。

２．Prdx1 欠損マウス結核感染モデルによる新規宿主防御遺伝子の同定

C57BL/6 と BALB/c の系統間では、結核菌に対する著しい感受性の違いがある。結核菌に抵抗性である Prdx1$^{-/-}$-B6 と感受性である Prdx1$^{-/-}$- BALB/c を交配した F1 は、結核菌に抵抗性であることがわかった。F1 と Prdx1$^{-/-}$-BALB/c の交雑群を作成し、結核菌の感染実験を行った。体重減少および致死を指標に、交雑群の連鎖解析を行った結果、マウス第 1 染色体に有意（P=0.0094）な連鎖が見られた。第 1 染色体に存在する結核菌抵抗性遺伝子座を、Prdx1$^{-/-}$-BALB/c に導入したコンジェニック系統を作製しており、現在 N6 世代（100% Prdx1$^{-/-}$-BALB/c に置換）を作製した。今後、樹立したコンジェニック系統の結核菌感染後の体重変化、生存日数等を指標に第 1 染色体に存在する結核菌抵抗性遺伝子を同定する。

課題番号　　：24 指 103
研究課題名　：マウス結核感染実験による結核ワクチン評価系構築
主任研究者名：切替　照雄
分担研究者名：舩渡川　圭次
キーワード　：結核感染実験、ワクチン、マウス
研究成果　：

【目的】新規の結核ワクチンを開発するためには、新たな病原因子を同定することが必須である。本研究では、結核菌強毒株 Erdman 由来 NCGM2242 株のマウス感染実験を実施し、その病原性を評価する。また、NCGM2242 株のワクチン効果を検証する。宿主防御因子候補分子 Peroxiredoxin1（Prdx1）のノックアウトマウスに結核菌を感染させ、結核菌に対する感受性を評価する。結核菌感染で発現が増加する宿主 microRNA155 のノックアウトマウスが結核感受性かどうか調べる。

【方法】感染実験に供する結核菌は、標準株 Erdman 株、NCGM2242 株を用いた。マウスは、C57BL/6 野生マウス、BALB/c 野生マウスおよび BALB/c をバックグラウンドに持つ Prdx1 ノックアウトマウス（Prdx1-/-, BALB/c マウス）の雄、８週齢を準備した。対数増殖期まで培養した結核菌を遠心して回収し、PBS で洗い、1×10^7 CFU/ml になるよう調製した。マウスの尾静脈より結核菌（2×10^6 CFU）を感染させた。感染させたマウスは、P3A 施設内のケージで飼育した。ワクチン効果を検証する場合は、接種菌量を $2\times10^{5.4}$CFU にし、接種１ヶ月後、Erdman 株（$2\times10^{5.4}$ CFU）を感染させた。

【結果】NCGM 2242 株の LD50 試験：NCGM 2242 株の LD50 を決定するため、2×10^7 生菌数を BALB/c マウスの腹腔に接種したが、300 日経過しても全て生存した。これに対して、Erdman 株を感染させた群では、平均 114 日（2×10^5 生菌数接種群）、136 日（2×10^4 生菌数接種群）、236 日（2×10^3 生菌数接種群）生存した。NCGM2242 株のワクチン効果試験（１）：NCGM2242 株のワクチン効果を検証するため、NCGM2242 株の生菌及び死菌を BALB/c マウスに接種し、４週後 Erdman 株を感染させた。何も接種しなかったコントロール群、および NCGM 2242 死菌を接種した群は、平均 44 日生存したのに対し、NCGM2242 生菌を接種した群は、平均 102 日生存した。NCGM2242 株のワクチン効果試験（２）：NCGM2242 株のワクチン効果を BCG と比較するため、NCGM 2242 株及び BCG を BALB/c マウスに接種し、４週後 Erdman 株を感染させた。何も接種しないコントロール群は、平均 129 日で死亡した。BCG を接種した群は、平均 161 日（2×10^3 生菌数接種群）もしくは 190 日（2×10^4 生菌数接種群）生存した。それに対して、NCGM 2242 株を接種した群は、平均 245 日（2×10^3 生菌数接種群）もしくは 258 日（2×10^4 生菌数接種群）生存した。

全ゲノムシークエンスにより、NCGM2242 株は *rrs*（別名 MTB000019 遺伝子）が変異していることがわかった（*rrs* の相補実験を計画中）。また、この変異により NCGM2242 株はカナマイシン耐性およびハイグロマイシン耐性になった。

Prdx1 ノックアウトマウスおよび miR-155 ノックアウトマウスは結核菌に感受性が高まっていた。また、BALB/c バックグラウンドの Prdx1 ノックアウトマウスも結核感受性であった。

【考察・結論】NCGM2242 株のワクチン効果：NCGM2242 株の生菌でワクチン効果が見られた。それに対し、熱で処理した死菌ではワクチン効果は、ほとんど見られなかった。死菌は、マウスの体内ですぐ処理されてしまい免疫が成立しない。

NCGM2242 株のリボソーム変異を相補（コンプリメント）する追加実験が必要になった。NCGM2242 株はリボソーム変異により複数の抗生物質耐性になったため、ゼオシンの耐性マーカーを有するプラスミドを構築した。このプラスミドへ *rrs* 発現に必要なオペロン領域８kbp を挿入しコンプリメント用プラスミドを得た。このプラスミドを NCGM2242 株に導入し、NCGM2242 の *rrs* 変異が回復することでワクチン効果などに影響があるかどうか調べる必要がある。

miR-155 は結核菌感染で発現が増加していた。miR-155 ノックアウトマウスは Th2 優位であり Th1 応答が正常ではなかったため結核菌への抵抗性が著しく低下していた。

研究発表及び特許取得報告について

課題番号：　24指103

研究課題名：　新しい病原因子を標的とした結核ワクチンの開発

主任研究者名：　切替　照雄

論文発表

論文タイトル	著者	掲載誌	掲載号	年
A silent mutation of mabG1 confers isoniazid resistance on Mycobacterium tuberculosis.	Ando H, Miyoshi-Akiyama T, Watanabe S, Kirikae T	Mol Microbiol	91(3)	2014
Differential function of Themis CABIT domains during T cell development.	Okada T, Nitta T, Kaji K, Takashima A, Oda H, Tamehiro N, Goto M, Okamura T, Patrick MS and Suzuki H.	PLoS One	9: e89115	2014
Zfat-Deficiency Results in a Loss of CD3ζ Phosphorylation with Dysregulation of ERK and Egr Activities Leading to Impaired Positive Selection.	*Ogawa, M., *Okamura, T., Ishikura, S., Doi, K., Matsuzaki, H., Tanaka, Y., Ota, T., Hayakawa, K., Suzuki, H., Tsunoda, T., Sasazuki, T. and Shirasawa, S.*The authors equally contributed to this work.	PLoS One	8, e76254	2013

学会発表

タイトル	発表者	学会名	場所	年月
A silent mutation in mabA confers isoniazid resistance on *Mycobacterium tuberculosis*.	安藤弘樹, 秋山徹, 渡邊真弥, 切替照雄	第87回日本細菌学会総会	東京	2014年3月
16S リボソーム RNA の解読領域の変異は結核菌を弱毒化する	舩渡川圭次, 渡邊真弥, 祝弘樹, 酘島由二, 奥村香世, 加藤雅子, 橋本雅仁, 切替富美子, 秋山徹, 切替照雄	第87回日本細菌学会総会	東京	2014年3月
Peroxiredoxin 1 contributes to host defense against *Mycobacterium tuberculosis*.	松村和典, 祝弘樹, 加藤雅子, 舩渡川圭次, 切替富美子, 秋山徹, 切替照雄	第87回日本細菌学会総会	東京	2014年3月
Peroxiredoxin 1 contributes to host defense against Mycobacterium tuberculosis.	松村和典, 祝弘樹, 加藤雅子, 舩渡川圭次, 切替富美子, 秋山徹, 切替照雄	第87回日本細菌学会総会	東京	2014年3月

研究発表及び特許取得報告について

その他発表(雑誌、テレビ、ラジオ等)

タイトル	発表者	発表先	場所	年月日
該当なし				

特許取得状況について　※出願申請中のものは(　　)記載のこと。

発明名称	登録番号	特許権者(申請者) (共願は全記載)	登録日(申請日)	出願国
結核菌の菌株の同定方法及び遺伝子変異の検出方法	PCT/JP2014/051208	秋山　徹、切替照雄、奥村香世	2014年1月22日	国際出願

※該当がない項目の欄には「該当なし」と記載のこと。
※主任研究者が班全員分の内容を記載のこ

OPEN ACCESS Freely available online

PLOS ONE

Zfat-Deficiency Results in a Loss of CD3ζ Phosphorylation with Dysregulation of ERK and Egr Activities Leading to Impaired Positive Selection

Masahiro Ogawa[1,2☯], Tadashi Okamura[3☯], Shuhei Ishikura[1,2], Keiko Doi[1,2], Hiroshi Matsuzaki[1], Yoko Tanaka[1], Takeharu Ota[1,2], Kunihiro Hayakawa[4], Harumi Suzuki[4], Toshiyuki Tsunoda[1,2], Takehiko Sasazuki[5], Senji Shirasawa[1,2]*

1 Department of Cell Biology, Faculty of Medicine, Fukuoka University, Jonan-ku, Fukuoka, Japan, **2** Central Research Institute for Advanced Molecular Medicine, Fukuoka University, Jonan-ku, Fukuoka, Japan, **3** Division of Animal Models, Department of Infectious Diseases, Research Institute, National Center for Global Health and Medicine, Tokyo, Japan, **4** Department of Immunology and Pathology, National Institute for Global Health and Medicine, Chiba, Japan, **5** Institute for Advanced Study, Kyushu University, Fukuoka, Japan

Abstract

The human *ZFAT* gene was originally identified as a susceptibility gene for autoimmune thyroid disease. Mouse Zfat is a critical transcriptional regulator for primitive hematopoiesis and required for peripheral T cell homeostasis. However, its physiological roles in T cell development remain poorly understood. Here, we generated *Zfat*$^{f/f}$*-LckCre* mice and demonstrated that T cell-specific *Zfat*-deletion in *Zfat*$^{f/f}$*-LckCre* mice resulted in a reduction in the number of CD4$^+$CD8$^+$double-positive (DP) cells, CD4$^+$single positive cells and CD8$^+$single positive cells. Indeed, in *Zfat*$^{f/f}$*-LckCre* DP cells, positive selection was severely impaired. Defects of positive selection in *Zfat*-deficient thymocytes were not restored in the presence of the exogenous TCR by using TCR-transgenic mice. Furthermore, *Zfat*-deficient DP cells showed a loss of CD3ζ phosphorylation in response to T cell antigen receptor (TCR)-stimulation concomitant with dysregulation of extracellular signal-related kinase (ERK) and early growth response protein (Egr) activities. These results demonstrate that Zfat is required for proper regulation of the TCR-proximal signalings, and is a crucial molecule for positive selection through ERK and Egr activities, thus suggesting that a full understanding of the precise molecular mechanisms of Zfat will provide deeper insight into T cell development and immune regulation.

Citation: Ogawa M, Okamura T, Ishikura S, Doi K, Matsuzaki H, et al. (2013) *Zfat*-Deficiency Results in a Loss of CD3ζ Phosphorylation with Dysregulation of ERK and Egr Activities Leading to Impaired Positive Selection. PLoS ONE 8(10): e76254. doi:10.1371/journal.pone.0076254

Editor: Troy A Baldwin, University of Alberta, Canada

Received May 10, 2013; **Accepted** August 22, 2013; **Published** October 3, 2013

Funding: This work was supported in part by a Grant-in-Aid for Scientific Research (B) from the Japan Society for the Promotion of the Science and a Grant-in-Aid for the FCAM from the Ministry of Education, Culture, Sports, Science, and Technology, Japan. The funders had no role in study design, data collection and analysis, decision to publish, or preparation of the manuscript.

Competing Interests: The authors have declared that no competing interests exist.

* E-mail: sshirasa@fukuoka-u.ac.jp

☯ These authors contributed equally to this work.

Introduction

ZFAT was originally identified as a candidate susceptibility gene for autoimmune thyroid disease [1]. *ZFAT* contains 18 zinc-finger domains and one AT-hook and is an evolutionally conserved gene from fish to humans, and the Zfat protein is highly expressed in the thymus and the spleen in adult mice [2]. We previously reported that *Zfat*-deficient (*Zfat*$^{-/-}$) mice are embryonic lethal by embryonic day 8.5, and Zfat is a critical transcriptional regulator for primitive hematopoiesis [3], and that ZFAT is functionally involved in the regulation of apoptosis of mouse embryonic fibroblasts and MOLT−4 cells [4,5].

Just recently, we generated *Zfat*$^{f/f}$*-Cd4Cre* mice [6], and showed that *Zfat*-deficient mice exhibited a reduction in the number of peripheral T cells with decreased surface expression of IL-7Rα and T cell antigen receptor (TCR)-stimulation-induced expression of CD25 and IL-2, indicating that Zfat is required for peripheral T cell homeostasis [6]. On the other hand, genetic variants of *ZFAT* have also been reported to be associated with adult height in Japanese and Korean population [7,8] and several common diseases including hypertension and cancer [9,10]. Of great interest is that a genetic variant of *ZFAT* is reported to be strongly associated with interferon-β responsiveness in multiple sclerosis [11] and the severity of Hashimoto's disease [12]. However, the exact functions of ZFAT during T cell development remain unknown.

T cells must be reactive to foreign pathogens, but tolerant to self-antigens. These features are formed during T cell development in the thymus [13]. CD4$^+$CD8$^+$double-positive (DP) cells expressing complete αβTCR complexes undergo positive selection, for differentiation into mature CD4$^+$single positive (CD4SP) cells or CD8$^+$single positive (CD8SP) cells [14–16]. DP cells that recognize self-peptide and major histocompatibility complex (pMHC) molecules with low affinities receive survival signals and differentiate into mature single positive cells; this process is known as positive selection. Accumulating evidence suggests that mitogen-activated protein kinase (MAPK) signaling pathways and the molecules in this pathway play critical roles in the regulation of the

cellular fate during T cell development [17]. Extracellular signal-related kinase (ERK) is activated by phosphorylation through sequential activation of Ras, Raf and MEK transduced by TCR-stimulation, and proper ERK activation is essential for positive selection [18–20].

Egr1, Egr2 and Egr3 are zinc-finger transcription factors of the early growth response protein (Egr) family, and they are rapidly induced in response to TCR-stimulation [21–23]. *Egr1*- or *Egr2*-deficiency was reported to result in defects of positive selection and survival of T cells [24,25]. *Egr3*-deficiency was reported to cause the impaired proliferation of thymocytes during transition from DN to DP cells [26]. Thus, TCR-stimulation-induced Egr expression is thought to be essential for the proper progression of T cell development in the thymus.

In this study, we generated *Zfat*$^{f/f}$-*LckCre* mice and showed that they exhibited a loss of CD3ζ phosphorylation with dysregulation of ERK and Egr activities leading to impaired positive selection. This is the first report demonstrating that Zfat is required for proper regulation of the TCR-proximal signalings, and is a crucial molecule for positive selection in the thymus.

Results

Reduction in the Number of Thymic DP, CD4SP and CD8SP cells in *Zfat*$^{f/f}$-*LckCre* Mice

To clarify the physiological roles of Zfat in T cell development in the thymus, we crossed *Zfat*$^{f/f}$ mice [6] with *LckCre* transgenic mice. The deletion of Zfat in *Zfat*$^{f/f}$-*LckCre* thymocytes was confirmed by an immunoblot analysis. While Zfat was detected specifically in the nuclear fraction of *Zfat*$^{f/f}$ thymocytes, the protein was hardly observed in *Zfat*$^{f/f}$-*LckCre* thymocytes (Figure 1A), indicating the efficient deletion of Zfat in the thymocytes of *Zfat*$^{f/f}$-*LckCre* mice. During the transition of DN stages in the *Zfat*$^{f/f}$ mice, the Zfat expression levels in the DN1 ($CD25^-CD44^+$) and DN2 ($CD25^+CD44^+$) subsets was low, whereas Zfat expression in the DN3 ($CD25^+CD44^-$), DN4 ($CD25^-CD44^-$) and DP subsets was detected at a higher level (Figure 1B). In contrast, in *Zfat*$^{f/f}$-*LckCre* mice, Zfat expression in the DN3 subset was slightly decreased compared with that of *Zfat*$^{f/f}$ mice, whereas Zfat expression in DN4 and DP subsets was apparently decreased compared with that of *Zfat*$^{f/f}$ mice (Figure 1B). These results indicated that the Zfat expression in *Zfat*$^{f/f}$-*LckCre* mice was abolished at the DN4 stage.

In *Zfat*$^{f/f}$-*LckCre* mice, the proportions of CD4SP and CD8SP cells, but not DP cells, were remarkably reduced and the total number of thymocytes, DP cells, CD4SP cells and CD8SP cells was significantly decreased compared with that of *Zfat*$^{f/f}$ mice (Figure 1C, 1D). On the other hand, the proportion and total number of DN cells in *Zfat*$^{f/f}$-*LckCre* mice seemed to be slightly increased compared with those of *Zfat*$^{f/f}$ mice, however, the difference of the total number of DN cells was not statistically significant (Figure 1C, 1D). Consistent with the decreased proportions and total number of CD4SP and CD8SP cells in the *Zfat*$^{f/f}$-*LckCre* thymus, a reduction in the proportion of $TCR\beta^+$T cells in both the spleen and lymph nodes (LNs) was observed in *Zfat*$^{f/f}$-*LckCre* mice (Figure 1E). The proportion and the total number of $CD4^+$or $CD8^+$T cells in the spleen and LNs were significantly reduced in *Zfat*$^{f/f}$-*LckCre* mice in comparison to those of *Zfat*$^{f/f}$ mice (Figure 1E, 1F). These results demonstrated that *Zfat*-deficiency results in impaired T cell development in the thymus.

In the thymus, a slight reduction in the expression levels of IL-7Rα on CD4SP and CD8SP cells in *Zfat*$^{f/f}$-*LckCre* mice was observed compared with those from *Zfat*$^{f/f}$ mice (Figure S1A). However, a difference in the expression levels of Bcl-2, a pro-survival factor induced by IL-7-mediated signaling [27,28], was not observed between the genotypes (Figure S1B), suggesting that the reduced expression of IL-7Rα did not play a functionally significant role in the reduction of T cells in the thymus of *Zfat*$^{f/f}$-*LckCre* mice.

Zfat-deficiency did not Affect the Transition of thymic DN to DP Cells

As the proportion and number of DN cells in *Zfat*$^{f/f}$-*LckCre* mice seemed to be slightly increased compared with those of *Zfat*$^{f/f}$ mice (Figure 1C, 1D), we next analyzed whether *LckCre*-mediated *Zfat*-deficiency would affect the T cell development at the DN stage. The proportions and total numbers of the DN subsets, i.e., DN1, DN2, DN3 and DN4, in *Zfat*$^{f/f}$-*LckCre* mice did not show significant differences with those of *Zfat*$^{f/f}$ mice, although the total numbers of DN3 and DN4 subsets seemed to be slightly elevated in *Zfat*$^{f/f}$-*LckCre* mice (Figure 2A, 2B). At the DN3 stage, thymocytes undergo β-selection through the pre-TCR signaling, leading to the transition from DN3a ($CD25^+CD44^-CD27^{lo}FSC^{lo}$) to DN3b ($CD25^+CD44^-CD27^{hi}FSC^{hi}$) cells [29,30]. The proportion of DN3b cells was comparable between the genotypes (Figure 2C), and the expression levels of intracellular TCRβ (icTCRβ) in *Zfat*$^{f/f}$-*LckCre* mice were comparable to those of *Zfat*$^{f/f}$ mice during the transition from the DN3 ($CD25^+$icTCRβ^+) to DN4 ($CD25^-$icTCRβ^+) stage (Figure 2D), which together indicated that the thymocytes in *Zfat*$^{f/f}$-*LckCre* mice normally passed through β-selection and transition from DN3 to DN4 cells.

We then addressed the transition from the DN4 to DP stage by analyzing an *ex vivo* culture system using Tst-4/DLL1 cells, which can support T cell development to the DP stage [31]. DN4 cells were sorted and then cultured on a monolayer of Tst-4/DLL1 cells. After 3 days of the culture, we confirmed a decline in Zfat expression in the thymocytes sorted from *Zfat*$^{f/f}$-*LckCre* thymus (Figure 2E), and observed the comparable proportions of the production of DP cells between *Zfat*$^{f/f}$ and *Zfat*$^{f/f}$-*LckCre* thymocytes (Figure 2F), indicating no blockade of the transition of DN4 to DP cells in *Zfat*$^{f/f}$-*LckCre* mice. Taken together, *Zfat*-deficiency did not affect the transition of thymic DN to DP cells including β-selection and transitions from DN3 to DN4 cells, and from DN4 to DP cells. In agreement with a decrease in DP cells *in vivo* (Figure 1D), however, the total number of the produced DP cells of *Zfat*$^{f/f}$-*LckCre* mice in *ex vivo* culture system was significantly reduced compared with that of *Zfat*$^{f/f}$ mice (Figure 2G), suggesting that there may be a defect in the proliferation or survival during the transition from DN to DP stage in the *Zfat*-deficient thymocytes.

Impaired Positive Selection in Thymocytes of *Zfat*$^{f/f}$-*LckCre* Mice

Loss of Zfat did not affect the DN to DP transition, in spite of significant reduction in the number of DP cells. We next analyzed an involvement of Zfat in positive selection of the DP cells. During the positive selection, $TCR\beta^{int}CD69^-$ DP cells initially show a $TCR\beta^{int}CD69^+$transitional phenotype (P-I; Figure 3A) after the TCR/pMHC interaction. After the positive selection, P-I cells become $TCR\beta^{hi}CD69^+$cells (P-II; Figure 3A) and then differentiate into CD4SP or CD8SP cells ($TCR\beta^{hi}CD69^-$) (P-III; Figure 3A) [20]. A considerable reduction in the proportion of P-I cells in thymocytes (1.4% versus 3.87%, respectively, Figure 3A) and DP cells (1.65% versus 4.35%, respectively, Figure 3B) from *Zfat*$^{f/f}$-*LckCre* mice was observed compared with that of *Zfat*$^{f/f}$ mice, indicating the existence of impaired positive

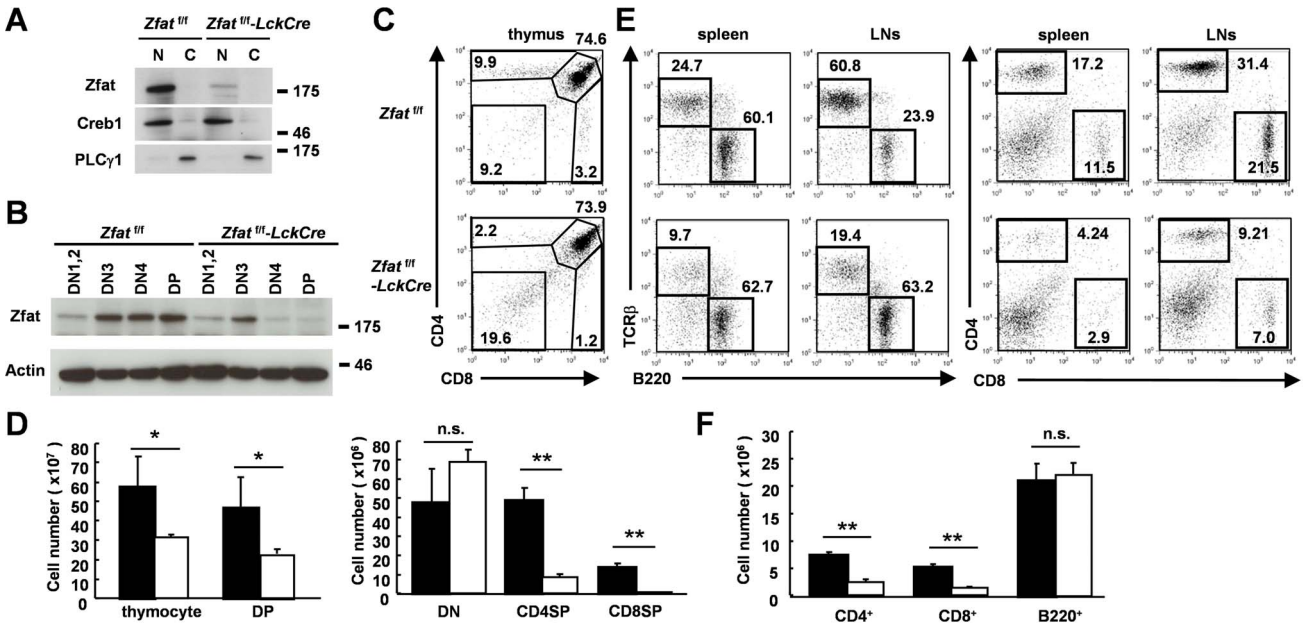

Figure 1. Reduction in the number of thymocytes and peripheral T cells in *Zfat*$^{f/f}$-*LckCre* mice. (A) An immunoblot of Zfat in nuclear (N) or cytoplasmic (C) fractions of thymocytes from *Zfat*$^{f/f}$ and *Zfat*$^{f/f}$-*LckCre* mice. CREB1 and PLCγ1 were used as controls of nuclear and cytoplasmic fractions, respectively. (B) An immunoblot of Zfat in DN1 and DN2 (DN1,2: CD4$^-$CD8$^-$CD44$^+$), DN3 (CD4$^-$CD8$^-$CD25$^+$CD44$^-$), DN4 (CD4$^-$CD8$^-$CD25$^-$CD44$^-$) or DP thymocytes from *Zfat*$^{f/f}$ and *Zfat*$^{f/f}$-*LckCre* mice. Actin was used as a loading control. (C) Flow cytometry analysis of the surface expression of CD4 and CD8 on thymocytes from *Zfat*$^{f/f}$ (top) and *Zfat*$^{f/f}$-*LckCre* (bottom) mice at 6 to 7 weeks of age. Data are representative of three independent experiments. (D) Total numbers of thymocytes, thymic DP, DN, CD4SP or CD8SP cells from *Zfat*$^{f/f}$ (black bars) and *Zfat*$^{f/f}$-*LckCre* (white bars) mice at 6 to 7 weeks of age. The data are the mean ± standard deviation (s.d.); $n=6$; * $P<0.05$; ** $P<0.01$; n.s., not significant. (E) Flow cytometry analysis of TCRβ$^+$T cells and B220$^+$B cells (left) or CD4$^+$and CD8$^+$T cells (right) in the spleen and LNs of *Zfat*$^{f/f}$ (top) and *Zfat*$^{f/f}$-*LckCre* (bottom) mice. Data are representative of three independent experiments. (F) Total numbers of CD4$^+$T, CD8$^+$T or B220$^+$B cells in the spleen from *Zfat*$^{f/f}$ (black bars) and *Zfat*$^{f/f}$-*LckCre* (white bars) mice. The data are the mean ± s.d.; $n=6$; ** $P<0.01$; n.s., not significant.
doi:10.1371/journal.pone.0076254.g001

selection in the *Zfat*-deficient DP thymocytes. However, no obvious alterations in the rearrangements of TCRαchains (Figure S2), the surface expression of TCRβ (Figure 3C) and CD45 (Figure 3D) [32] on DP thymocytes were observed between the genotypes. In addition, the expression levels of CD5, which is known to be correlated with the avidity of TCR/pMHC

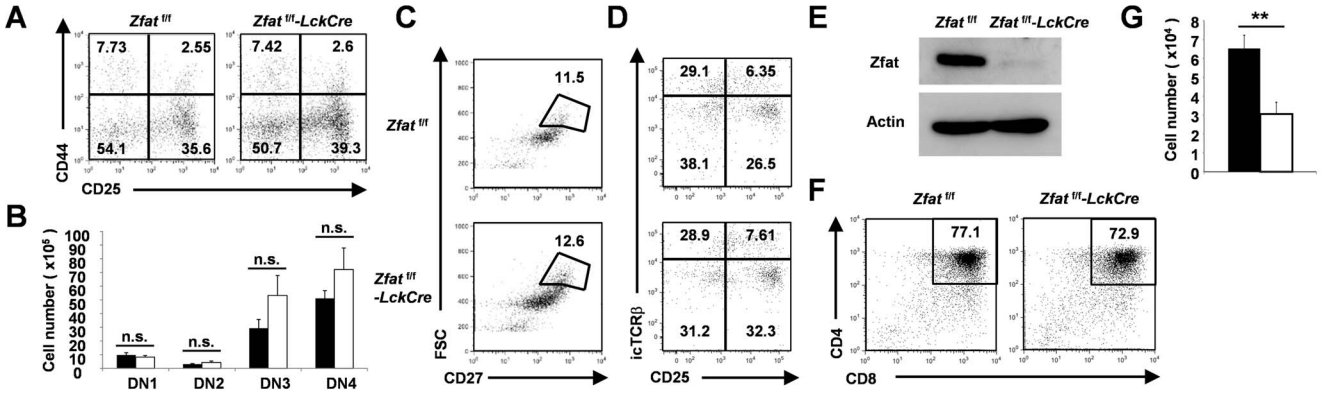

Figure 2. *Zfat*-deficiency did not affect the transition of thymic DN3 to DP cells. (A) Flow cytometry analysis of the surface expression of CD44 and CD25 on CD4$^-$CD8$^-$ DN thymocytes from *Zfat*$^{f/f}$ and *Zfat*$^{f/f}$-*LckCre* mice at 6 to 7 weeks of age. The numbers in the quadrants indicate the percent DN1 (upper left), DN2 (upper right), DN3 (lower right) or DN4 (lower left) subsets in DN thymocytes from the indicated genotypes. Data are representative of three independent experiments. (B) Total numbers of DN1, DN2, DN3 or DN4 cells from *Zfat*$^{f/f}$ (black bars, $n=3$) and *Zfat*$^{f/f}$-*LckCre* (white bars, $n=3$) mice at 6 to 7 weeks of age. The data are the mean ± standard deviation (s.d.); n.s., not significant. (C) Flow cytometry analysis of the surface expression of CD27 and forward scatter (FSC) of DN3 thymocytes. The gated area indicates DN3b (CD27^{hi}FSC^{hi}) subsets. Data are representative of three independent experiments. (D) Flow cytometry analysis of TCRβ-negative DN (CD4$^-$CD8$^-$TCRβ$^-$) cells. The intracellular expression of TCRβ (icTCRβ) and surface expression of CD25 are shown. Data are representative of three independent experiments. (E-G) Sorted DN4 cells were co-cultured with Tst-4/DLL1 cells for 3 days and analyzed by an immunoblot of Zfat (E) and flow cytometry for the surface expression of CD4 and CD8 (F). The proportions (F) or total numbers (G) of CD4$^+$CD8$^+$DP thymocytes from *Zfat*$^{f/f}$ (top, black bar, $n=3$) or *Zfat*$^{f/f}$-*LckCre* (bottom, white bar, $n=3$) mice are shown. The data are the mean ± standard deviation (s.d.); ** $P<0.01$. * $P<0.05$.
doi:10.1371/journal.pone.0076254.g002

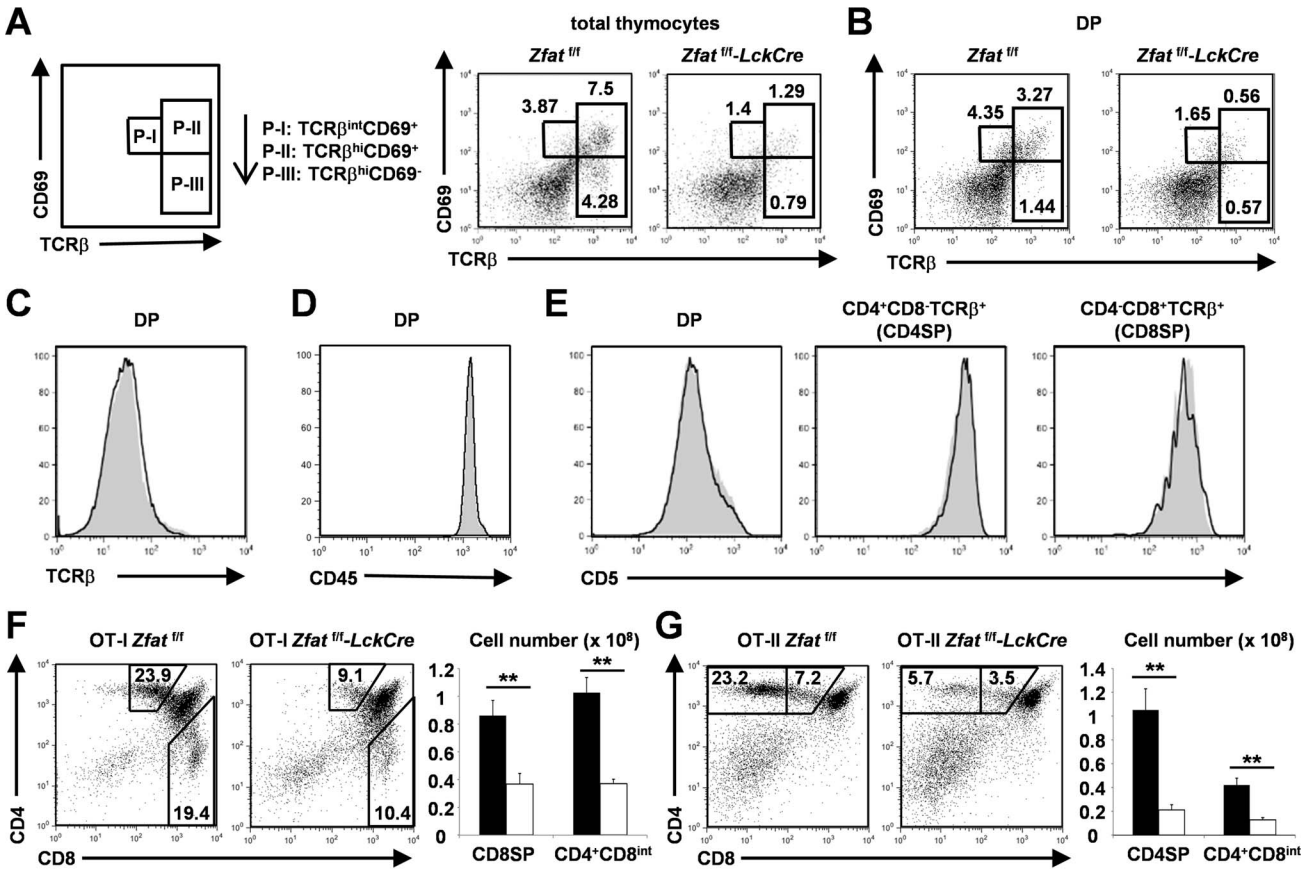

Figure 3. Impaired positive selection in *Zfat*$^{f/f}$-*LckCre* thymus. (A, B) A scheme of the intermediates of positive selection defined by changes in expression of TCRβ and CD69: TCRβ^{int}CD69^{+}(P-I), TCRβ^{hi}CD69^{+}(P-II) and TCRβ^{hi}CD69^{-} (P-III) are generated sequentially as shown by arrows (A, left). Flow cytometry analysis of the surface expression of CD69 and TCRβ on total thymocytes (A) or DP cells (B) from the indicated genotypes at 6 to 7 weeks of age. The numbers indicate the proportion of the gated area. Data are representative of three independent experiments. (C-E) Surface expression of TCRβ on DP cells (C), CD45 on DP cells (D) or CD5 on DP, CD4^{+}CD8^{-}TCRβ^{+}or CD4^{-}CD8^{+}TCRβ^{+}cells (E) from *Zfat*$^{f/f}$ (gray-filled) and *Zfat*$^{f/f}$-*LckCre* (black line) mice at 6 to 7 weeks of age. Data are representative of three independent experiments. (F, G) Flow cytometry analysis for the surface expression of CD4 and CD8 on the thymocytes and total numbers of CD4^{+}CD8^{int}, CD8SP or CD4SP cells from OT-I *Zfat*$^{f/f}$ (black bar) and OT-I *Zfat*$^{f/f}$-*LckCre* mice (white bar) (F) or from OT-II *Zfat*$^{f/f}$ (black bar) and OT-II *Zfat*$^{f/f}$-*LckCre* mice (white bar) (G). The numbers indicate the proportion of the gated area. The data are the mean ± standard deviation (s.d.); $n = 3$; ** $P < 0.01$. Data are representative of three independent experiments.
doi:10.1371/journal.pone.0076254.g003

interaction [33], on DP, CD4SP and CD8SP cells were comparable between the genotypes (Figure 3E). These results strongly indicated that the αβTCR recombination and TCR/pMHC avidity are normal during T cell development in *Zfat*$^{f/f}$-*LckCre* mice.

To further confirm the impaired positive selection in *Zfat*$^{f/f}$-*LckCre* mice, we crossed ovalbumin (OVA)-specific MHC class I-restricted TCR transgenic (OT-I) [34] or MHC class II-restricted TCR transgenic mice (OT-II) [35] with *Zfat*$^{f/f}$-*LckCre* mice, and examined the developmental fate of thymocytes in OT-I *Zfat*$^{f/f}$-*LckCre* and OT-II *Zfat*$^{f/f}$-*LckCre* mice. It is known that DP cells pass through the CD4^{+}CD8^{int} transitional stage before complete differentiation into either CD4SP or CD8SP cells [14]. As expected, not only the proportions but also the total numbers of CD8SP and CD4^{+}CD8^{int} cells were significantly decreased in OT-I *Zfat*$^{f/f}$-*LckCre* mice compared with those of OT-I *Zfat*$^{f/f}$ mice (Figure 3F), suggesting that MHC class I-restricted positive selection in OT-I *Zfat*$^{f/f}$-*LckCre* mice was impaired. In addtion, MHC class II-restricted positive selection in OT-II *Zfat*$^{f/f}$-*LckCre* mice was also impaired, as both the proportions and the total numbers of CD4SP and CD4^{+}CD8^{int} cells were remarkably reduced in OT-II *Zfat*$^{f/f}$-*LckCre* compared with those of OT-II *Zfat*$^{f/f}$ mice (Figure 3G). Together, these results confirmed that positive selection is impaired in the *Zfat*-deficient thymocytes.

Zfat-deficiency Impaired CD3ζ Phosphorylation with Defects in ERK1/2 Activation

To elucidate mechanisms of the impaired positive selection observed in *Zfat*$^{f/f}$-*LckCre* DP cells, we examined phosphorylation of molecules working at the signaling transduced by TCR-stimulation. Phosphorylations of ERK1/2 induced by TCR-stimulation, which is known to be critical in the positive selection, were markedly decreased in *Zfat*$^{f/f}$-*LckCre* thymocytes compared with those of *Zfat*$^{f/f}$ thymocytes (Figure 4). In agreement with the defects in ERK1/2 activation, the phosphorylations of both MEK1/2 and c-Raf, which are located upstream of the ERK signaling pathway, were also reduced in the *Zfat*$^{f/f}$-*LckCre* thymocytes compared with those of *Zfat*$^{f/f}$ thymocytes (Figure 4). Furthermore, the phosphorylations of Zap70 and PLCγ1 were diminished in *Zfat*$^{f/f}$-*LckCre* thymocytes (Figure 4). Finally, TCR stimulation-induced phosphorylation of CD3ζ was virtually ablated in the *Zfat*$^{f/f}$-*LckCre* thymocytes, and the phosphorylated-CD3ζ at non-stimulated status was also apparently diminished due to the *Zfat*-deficiency (Figure 4). However, phosphorylated status

at Tyr505 of Lck, which phosphorylates tyrosine residues in ITAMs of CD3ζ in response to TCR-stimulation [36], was comparable between the genotypes. Taken together, these results indicate TCR signaling cascade is strikingly attenuated in *Zfat*$^{f/f}$-*LckCre* DP cells at CD3ζ phosphorylation concurrent with ERK1/2 phosphorylation. Moreover, the impaired positive selection in *Zfat*$^{f/f}$-*LckCre* DP cells is thought to be attributed to defects in the activation of ERK1/2 induced by TCR-stimulation.

TCR-stimulation-induced Egr Expressions were Impaired in the *Zfat*-deficient Thymocytes

Next, we examined the expression levels of Egr1, Egr2 and Egr3, which are known to be induced by TCR-stimulation. Both the Egr1 and Egr2 expressions were robustly increased in the *Zfat*$^{f/f}$ DP cells after the stimulation with anti-CD3ε and anti-CD28 antibodies *in vitro* (Figure 5A), whereas expression levels of both Egr1 and Egr2 in the *Zfat*$^{f/f}$-*LckCre* DP cells after the stimulation were not much induced compared with those of *Zfat*$^{f/f}$ DP cells. In addition, it appeared that the Egr1 expression level before the stimulation was also decreased in the *Zfat*$^{f/f}$-*LckCre* DP cells compared with that of the *Zfat*$^{f/f}$ DP cells (Figure 5A). On the other hand, Egr3 was constitutively expressed and slightly increased in the *Zfat*$^{f/f}$ DP cells after the stimulation, whereas the expression levels of Egr3 in the *Zfat*$^{f/f}$-*LckCre* DP cells were constitutively lower compared with those of *Zfat*$^{f/f}$ DP cells and rarely enhanced by TCR-stimulation (Figure 5A). These results indicated that *Zfat*-deficiency causes dysregulated expression of Egr protein in the DP cells before and after TCR-stimulation. Similar experiments were performed on the thymocytes from OT-II *Zfat*$^{f/f}$-*LckCre* mice. Phosphorylation of ERK induced by TCR-stimulation in the thymocytes from OT-II *Zfat*$^{f/f}$-*LckCre* mice was decreased compared with that of OT-II *Zfat*$^{f/f}$ mice (Figure S3A). Furthermore, the levels of TCR-stimulation-induced Egr1, Egr2 and Egr3 expression in OT-II *Zfat*$^{f/f}$-*LckCre* thymocytes were all decreased compared with those of OT-II *Zfat*$^{f/f}$ mice (Figure S3B), and together these findings suggested that the impaired phosphorylation of ERK and Egr expression induced by TCR-stimulation was caused by molecules other than TCR itself.

To address whether MEK activation is essential for ERK mediated Egr inductions under the TCR-stimulated condition, we stimulated DP cells in the presence of U0126, an inhibitor of MEK1/2 [37]. We found that the inductions of Egr1 and Egr2 were considerably reduced by the treatment with U0126 both in *Zfat*$^{f/f}$ and *Zfat*$^{f/f}$-*LckCre* DP cells (Figure 5B), indicating that the enhancements of Egr1 and Egr2 expression by TCR-stimulation were essentially regulated by the MEK-ERK axis. On the other hand, the Egr3 induction was just partly reduced by the treatment with U0126 in *Zfat*$^{f/f}$ DP cells, whereas the Egr3 expression in the *Zfat*$^{f/f}$-*LckCre* DP cells seemed to be slightly increased or unaltered by TCR-stimulation in the presence of U0126 (Figure 5B). These results suggested the possibility that Egr3 expression may be regulated by other signaling pathways in addition to the MEK-ERK pathway.

While the levels of *Egr* mRNA expression in the unstimulated DP cells were comparable between the *Zfat*$^{f/f}$ and *Zfat*$^{f/f}$-*LckCre* genotypes (Figure 5C), each of the *Egr1*, *Egr2* and *Egr3* mRNA inductions by TCR-stimulation were robustly suppressed in *Zfat*$^{f/f}$-*LckCre* DP cells compared with those of *Zfat*$^{f/f}$ DP cells (Figure 5D), suggesting that Zfat is required for proper *Egr* gene expression induced by TCR-stimulation. However, considering the fact that the expressions of Egr proteins were slightly decreased in the unstimulated *Zfat*$^{f/f}$-*LckCre* DP cells (Figure 5A), *Zfat*-deficiency might affect the turnover or degradation of Egr proteins as well as the expression of *Egr* mRNAs. Taken together, these results indicated that impairment of the TCR-stimulation-induced Egr inductions in the *Zfat*-deficient thymocytes leads to the defects of positive selection.

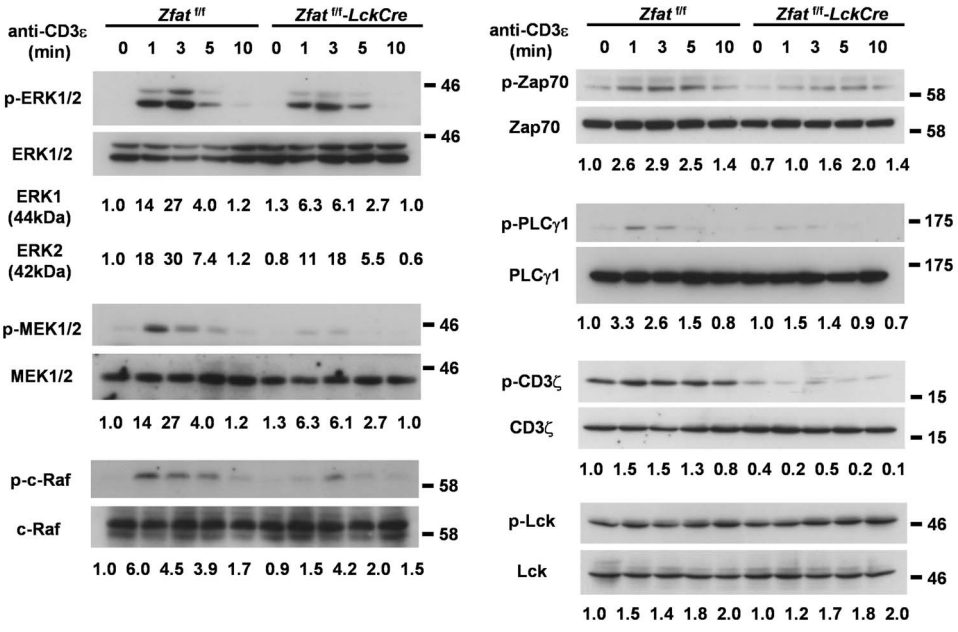

Figure 4. *Zfat*-deficiency impaired CD3ζ phosphorylation with defects in ERK1/2 activation. Immunoblots for phosphorylated or total protein of ERK, MEK1/2, c-Raf, Zap70, PLCγ1, CD3ζ and Lck before or at the indicated time points after the stimulation with cross-linking anti-CD3ε antibody in thymocytes from the indicated genotypes. The values below each image represent the relative ratio of the amount of phosphorylated protein to total protein. Data are representative of three independent experiments.
doi:10.1371/journal.pone.0076254.g004

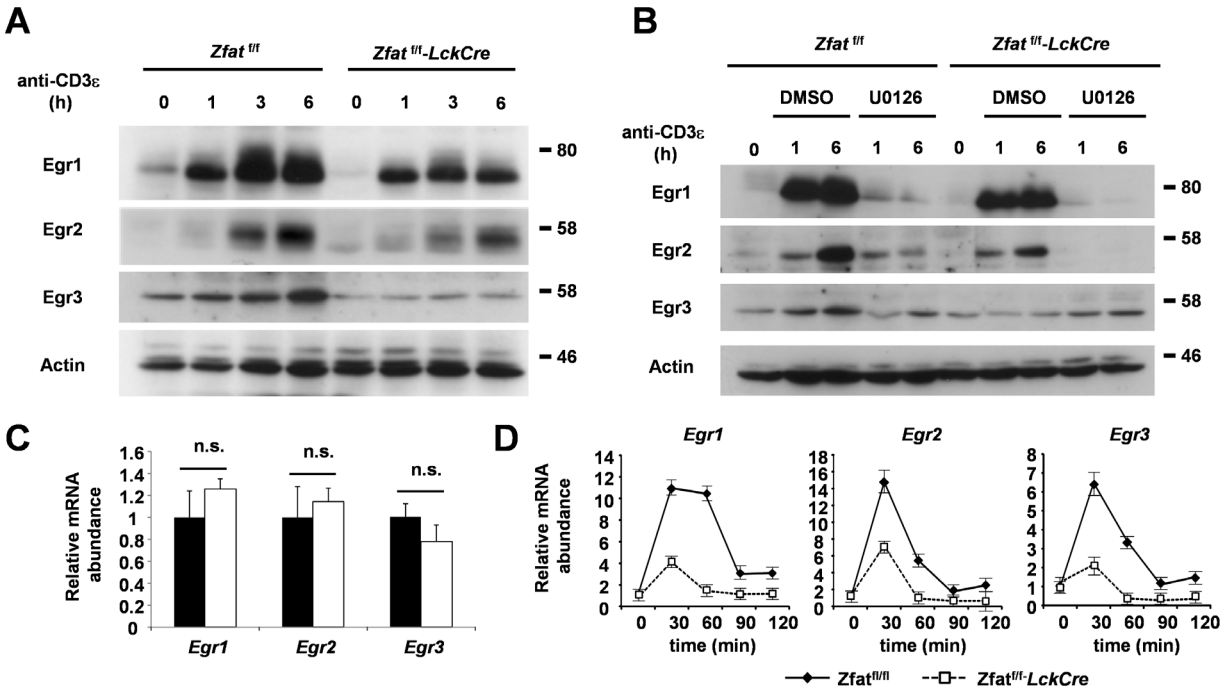

Figure 5. TCR-stimulation induced Egr expressions were impaired in the *Zfat*-deficient DP thymocytes. (A)Immunoblots for Egr1, Egr2 and Egr3 before or at the indicated time points after the stimulation with plate-bound anti-CD3ε and anti-CD28 antibodies in DP cells from the indicated genotypes. Actin was used as a loading control. Data are representative of three independent experiments. (B) Immunoblots for Egr1, Egr2 and Egr3 in DP cells from the indicated genotypes before or at the indicated time points after the stimulation with plate-bound anti-CD3ε and anti-CD28 antibodies under the condition with U0126 in DMSO or with DMSO alone. Actin was used as a loading control. Data are representative of three independent experiments. (C, D) Quantitative RT-PCR analysis of *Egr1*, *Egr2* and *Egr3* expression before (C) or at the indicated time points after the stimulation with anti-CD3ε and anti-CD28 antibodies (D) in DP cells from *Zfat*$^{f/f}$ and *Zfat*$^{f/f}$-*LckCre* mice. The relative expression for each gene was normalized by the expression of *Actb*. The results are presented as the value relative to the unstimulated DP cells from *Zfat*$^{f/f}$ mice. The data are the mean ± s.d.; n.s., not significant.
doi:10.1371/journal.pone.0076254.g005

Discussion

In this study, we demonstrated that Zfat is required for the proper phosphorylation of CD3ζ, and is a critical regulator for T cell development in the thymus, especially for positive selection. The molecular mechanism by which *Zfat*-deficiency leads to impaired positive selection would be mainly dependent on the loss of CD3ζphosphorylation leading to the impaired ERK activation transduced by TCR-stimulation. Furthermore, activated ERK-mediated expression of Egr1 and Egr2, which are critical regulators for positive selection, were also decreased in the *Zfat*$^{f/f}$-*LckCre* thymocytes. Taken together, these results suggest that Zfat is involved in the proper regulation of the TCR-proximal signalings, which is required for positive selection in the thymus.

Zfat$^{f/f}$-*LckCre* mice showed a considerable reduction in the number of DP thymocytes. We could not find apparent defects in T cell development at DN stage or transition of DN to DP cells in *Zfat*-deficient thymocytes *in vivo* and *ex vivo* experiments. Therefore, the reduction in the number of DP cells in *Zfat*$^{f/f}$-*LckCre* mice may be due to the *Zfat*-deficiency at the DP stage. However, Zfat expression was not completely abolished in the *Zfat*$^{f/f}$-*LckCre* DN3 thymocytes, and thus the possibility that Zfat is necessary for proper development at the DN stage cannot be excluded.

Impaired positive selection in *Zfat*-deficient thymocytes was not restored in the presence of OT-I TCR or OT-II TCR transgene, which promote positive selection and differentiation of DP cells into CD8SP or CD4SP cells. These results strongly indicated that positive selection is impaired in *Zfat*-deficient mice, and also suggested that the defect of positive selection is caused by the dysregulated signaling downstream of TCR itself. TCR-stimulation triggers activation of the ERK pathway through sequential activation of Ras, Raf and MEK [17]. Activation of ERK is critical in the TCR-mediated signaling cascades and an essential requirement for positive selection in the thymus [19,20].

Both Egr1 and Egr2 expression are critically regulated by activated ERK transduced by TCR-stimulation and play pivotal roles in positive selection and survival of DP cells [24,25,38]. Intriguingly, we identified the defects of TCR-stimulated ERK phosphorylation and Egr inductions in *Zfat*-deficient DP thymocytes, indicating that impaired Egr induction was at least partially responsible for the defects of positive selection in *Zfat*$^{f/f}$-*LckCre* mice. Moreover, Egr3 was also dysregulated in *Zfat*-deficient thymocytes. *Egr3*-deficient mice have been reported to exhibit a defect in the thymocytes proliferation and a partial block in differentiation at the DN3 stage [26]. Therefore, a possibility that Zfat plays an important role in the proliferation of thymocytes during the DN to DP transition through Egr3 induction is not excluded.

Decreased phosphorylation of CD3ζ in *Zfat*$^{f/f}$-*LckCre* thymocytes induced by TCR-stimulation was observed, indicating that *Zfat*-deficiency results in impaired activation of TCR signaling at proximal level. Tyrosines in ITAMs of CD3ζ are phosphorylated by Src family kinase Lck, and then the tyrosine-phosphorylated ITAMs of CD3ζ serve as docking sites for Zap70 in response to TCR stimulation [36]. However, *Zfat*-deficiency did not affect phosphorylation status of Lck in the thymocytes, whereas phosphorylation of Zap70 was reduced in *Zfat*$^{f/f}$-*LckCre* thymo-

cytes. We have not elucidated how exactly Zfat affects the CD3ζphosphorylation in this study. Activation of CD3ζ is negatively regulated by SHP−1 and SHP−2 (SH2 domain-containing phosphatase-1 and -2) through dephosphorylation [39,40]. Moreover, c-Cbl E3 ubiquitin ligase reduces CD3ζ levels at the plasma membrane by stimulating internalization [39,41]. Considering that Zfat is expected to be a transcriptional regulator in the nucleus [2,3], Zfat might affect the expressions of the genes involved in the regulation of CD3ζ phosphorylation, such as SHP-1, SHP-2 and c-Cbl. However, elucidation of the precise molecular mechanisms of Zfat function in regulation of TCR signaling should await future studies.

Proper activation of TCR signaling is also required for negative selection in the thymus. Thus, Zfat might be involved in the negative selection since *Zfat*-deficiency results in the defect in proximal molecules of TCR complex. However, we have not seen obvious differences in the T cell developments between H-Y $Zfat^{f/f}$ *and* H-Y $Zfat^{f/f}$-*LckCre* male mice in preliminarily experiments (data not shown). To establish a role for Zfat in the negative selection, further studies should be required in the future.

In conclusion, we demonstrated that *Zfat*-deficiency in DP cells results in a loss of CD3ζ phosphorylation with dysregulation of ERK and Egr activities leading to impaired positive selection in the thymus, suggesting that Zfat is a pivotal molecule in T cell development. As the activation of ERK-Egr pathway was not completely impaired in the *Zfat*-deficient thymocytes, the possibility that Zfat plays crucial roles in particular signaling pathways other than ERK-mediated pathway does exist. Thus, a full understanding of the roles and precise molecular mechanisms of the transcriptional regulator Zfat will lead to a better understanding of the orchestrated gene expression programs and provide deeper insight into T cell development, immune regulation and a wide variety of diseases.

Materials and Methods

Mice

$Zfat^{f/f}$ mice were originally generated as described previously [6] and backcrossed to a C57BL/6 background over seven generations. $Zfat^{f/f}$ mice were crossed to Lck-Cre mice from Taconic to generate T-cell-specific *Zfat* knockout ($Zfat^{f/f}$-*LckCre*) mice in the C57BL/6 background. All the animal experiments were approved by the Animal Care and Use Committee of the NCGM Research Institute, and the experiments on mice were carried out under the guidelines of the Institutional Animal Care and Use Committee of Fukuoka University.

Immunoblotting

The nuclear and cytoplasmic fractions from thymocytes were prepared using NE-PER Nuclear and Cytoplasmic Extraction Kit (Pierce). Separated cells were lysed in RIPA buffer [50 mM Tris-HCl, pH 7.5, 150 mM NaCl, 1% NP−40, 0.5% deoxycholate, 0.1% SDS, protease inhibitor cocktail (Roche)]. Equal amounts of total lysates were electrophoresed in 7, 8.5 or 4–20% SDS-polyacrylamide gels, and transferred to a nitrocellulose membrane (GE Healthcare). The antibodies used for immunoblotting analysis and their specificities were as follows: Egr3, phosphorylated ERK, antibodies for phosphorylated and total Zap70, PLCγ1, c-Raf, and Lck (all from Cell Signaling Technology); CREB1 (C-21), Erk (K-23) and Egr1 (C-19; all from Santa Cruz); total and phosphorylated MEK1/2 (from New England Biolabs); Actin (A2066; from Sigma); Egr2 (from Proteintech Group); CD3ζ (from Exbio); phosphorylated CD3ζ (A0468; from Assay biotech). Anti-Zfat antibody was prepared as described previously [2]. The horseradish peroxidase-conjugated secondary antibody (GE Healthcare) and SuperSignal West Pico Chemiluminescent Substrate (Thermo Scientific) were used for the detection. The quantitative analysis of the immunoblotting was done using the integration value of each blot with Image J software (version1.46, US National Institutes of Health) [42].

Flow Cytometry

Cells from the spleen, lymph nodes and the thymus were depleted of erythrocytes by hypotonic lysis and stained with fluorophore-conjugated antibodies. A Cytofix/Cytoperm kit (BD Biosciences) was used for analysis of the intracellular detection of TCRβ. Data were collected with a cytometer (FACSAria II; BD Biosciences) and analyzed with FlowJo software (Tomy Digital Biology). The fluorophore-conjugated antibodies used for flow cytometry analysis and their specificities were as follows: CD4 (RM4–5), CD8 (53-6.7), B220 (RA3-6B2), CD25 (PC61), CD44 (IM7), CD27 (LG.3A10), TCRβ (H57-597), CD69 (H1.2F3), CD45 (30-F11) and CD5 (53-7.3; all from Biolegend).

In vitro Differentiation of DN3 Cells

Tst-4/DLL1 stromal cells (RCB2118) were provided by the RIKEN BRC through the National Bio-Resource Project of the MEXT, Japan. Cells were plated and co-cultured with sorted DN4 ($CD4^-CD8^-CD25^-CD44^-$) cells. DN4 cells (1×10^5) were cultured at 37°C with 5% CO_2 in RPMI 1640 medium containing 10% FCS, penicillin-streptomycin-glutamine (Life Technologies) and β-mercaptoethanol (50 nM; Sigma) supplemented with recombinant mouse IL-7 (0.5 ng/ml; Pepro Tech) and SCF (1 μg/ml; R&D Systems).

In vitro TCR-stimulation

Thymocytes (1×10^7) from mice were stimulated at 37°C with anti-CD3ε antibody (10 μg/ml, 145-2C11; Biolegend) cross-linked with goat anti-hamster IgG (80 μg/ml; Southern Biotech) in RPMI 1640 medium containing 10% FCS, penicillin-streptomycin-glutamine (Life Technologies) and β-mercaptoethanol (50 nM; Sigma). For the stimulation with plate-bound anti-CD3ε and anti-CD28 antibodies, plates were coated overnight with anti-CD3ε (1 μg/ml) and anti-CD28 (3 μg/ml, 37.51; Biolegend) antibodies. DP cells (5×10^6) were stimulated with plate-bound anti-CD3ε and anti-CD28 antibodies under the condition with U0126 (100 μM; Calbiochem) in DMSO or with DMSO alone.

Quantitative RT-PCR

Total RNA was extracted by TRIZol reagent with PureLink RNA Mini Kit (Life Technologies). Superscript VILO cDNA synthesis kit (Life Technologies) was used for reverse transcription. Quantitative RT-PCR was performed by using Thunderbird SYBR qPCR Mix (TOYOBO) with ABI PRISM 7900HT (Applied Biosystems). The PCR primers used for *Egr1* 5′-AGGACTTGATTTGCATGGTATTGGA-3′ and 5′-ATG-CAGGGCAGGGTTCTGAG-3′, *Egr2* 5′-GAACCAGGA-CACCGTGAGATGA-3′ *and* 5′-GTAGTGTTGGCAGCTCG-GACAG-3′, *Egr3* 5′-GACTCGGTAGCCCATTACAATCAGA-3′ and 5′-GAGAGTTCCGGATTGGGCTTC-3′ and *Actin* 5′-CATCCGTAAAGACCTCTATGCCAAC-3′ and 5′-ATG-GAGCCACCGATCCACA-3′.

Statistical Analysis

Data are presented as the means ± s.d. and statistical analysis was performed using an unpaired Student's *t*-test when comparing

the means of two groups. Differences of $P<0.05$ were considered to be statistically significant (*$P<0.05$; **$P<0.01$).

Accession Number

GenBank mRNA sequences: Zfat, NT_078782.

Supporting Information

Figure S1 Surface expression of IL-7Rα and intracellular expression of Bcl-2. Flow cytometry analysis of the expression of surface IL-7Rα (A) and intracellular Bcl-2 (B) in the DP, CD4SP and CD8SP cells from *Zfat*$^{f/f}$ (gray-filled) and *Zfat*$^{f/f}$*-LckCre* (black line) mice at 6 to 7 weeks of age (left). Data of thymocytes from *Zfat*$^{f/f}$ (black bar) and *Zfat*$^{f/f}$*-LckCre* (white bar) mice were measured as the mean fluorescence intensity (MFI) (right). The fluorophore-conjugated antibodies used for flow cytometry analysis and their specificities were as follows: IL-7Rα (A7R34) and Bcl-2 (10C4; all from Biolegend). Data are representative of three independent experiments. The data are the mean ± s.d.; * $P<0.05$; ** $P<0.01$; n.s., not significant.
(TIF)

Figure S2 Rearrangements of TCRα chains in *Zfat*$^{f/f}$ or *Zfat*$^{f/f}$*-LckCre* thymocytes. Semiquantitative RT-PCR analysis of *Vα*-to-*Cα* rearrangements in DP thymocytes from the indicated genotypes. *Cα-Cα* amplification within a *Cα* region served as the control. *Gapdh*, an internal control. Primer sequences used for amplifications were as follows: *Vα3* 5′-CCCAGTGGTTCAAGGAGTGA-3′, *Vα6* 5′-CTGACTCATGTCAGCCTGAGAG-3′, *Vα8* 5′-CAACAAGAGGACCGAGCACC-3′, *Vα14* 5′-TGGGAGATACTCAGCAACTCTGG-3′, *Vα19* 5′-CTGCTTCTGACAGAGCTCCAG-3′ and *Cα* 5′-TTCAAAGAGACCAACGCCAC-3′ with *Cα* Rv primer 5′-TTCAGCAGGAGGATTCGGAG-3′, *Gapdh* Fw 5′-GAACGGATTTGGCCGTATTG-3′ and *Gapdh* Fw 5′-GATGATGACCCTTTTGGCTC-3′. Data are representative of three independent experiments.
(TIF)

Figure S3 Reduced ERK activation and Egr induction in OT-II *Zfat*$^{f/f}$*-LckCre* thymocytes. (A) Immunoblots for phosphorylated or total protein of ERK before or the indicated time points after the stimulation with cross-linking anti-CD3ε antibody in thymocytes from the indicated genotypes. The values below each image represent the relative ratio of the amount of phosphorylated protein to total protein. Data are representative of three independent experiments. (B) Immunoblots for Egr1, Egr2 and Egr3 before or at the indicated time points after the stimulation with plate-bound anti-CD3ε and anti-CD28 antibodies in DP cells from the indicated genotypes. Actin was used as a loading control. Data are representative of three independent experiments.
(TIF)

Acknowledgments

The authors thank Takahiro Fujimoto, Aya Fujikane, Masato Hamabashiri, Midori Koyanagi and Takami Danno for technical assistance.

Author Contributions

Conceived and designed the experiments: MO SS. Performed the experiments: MO KD HM YT T. Ota KH HS. Analyzed the data: MO SI TT. Contributed reagents/materials/analysis tools: T. Okamura TS SS. Wrote the paper: MO SI SS.

References

1. Shirasawa S, Harada H, Furugaki K, Akamizu T, Ishikawa N, et al. (2004) SNPs in the promoter of a B cell-specific antisense transcript, SAS-ZFAT, determine susceptibility to autoimmune thyroid disease. Hum Mol Genet 13: 2221–2231.
2. Koyanagi M, Nakabayashi K, Fujimoto T, Gu N, Baba I, et al. (2008) ZFAT expression in B and T lymphocytes and identification of ZFAT-regulated genes. Genomics 91: 451–457.
3. Tsunoda T, Takashima Y, Tanaka Y, Fujimoto T, Doi K, et al. (2010) Immune-related zinc finger gene ZFAT is an essential transcriptional regulator for hematopoietic differentiation in blood islands. Proc Natl Acad Sci U S A 107: 14199–14204.
4. Doi K, Fujimoto T, Koyanagi M, Tsunoda T, Tanaka Y, et al. (2011) ZFAT is a critical molecule for cell survival in mouse embryonic fibroblasts. Cell Mol Biol Lett 16: 89–100.
5. Fujimoto T, Doi K, Koyanagi M, Tsunoda T, Takashima Y, et al. (2009) ZFAT is an antiapoptotic molecule and critical for cell survival in MOLT−4 cells. FEBS Lett 583: 568–572.
6. Doi K, Fujimoto T, Okamura T, Ogawa M, Tanaka Y, et al. (2012) ZFAT plays critical roles in peripheral T cell homeostasis and its T cell receptor-mediated response. Biochem Biophys Res Commun. 425: 107–112.
7. Cho YS, Go MJ, Kim YJ, Heo JY, Oh JH, et al. (2009) A large-scale genome-wide association study of Asian populations uncovers genetic factors influencing eight quantitative traits. Nat Genet 41: 527–534.
8. Takeuchi F, Nabika T, Isono M, Katsuya T, Sugiyama T, et al. (2009) Evaluation of genetic loci influencing adult height in the Japanese population. J Hum Genet 54: 749–752.
9. Ramakrishna M, Williams LH, Boyle SE, Bearfoot JL, Sridhar A, et al. (2010) Identification of candidate growth promoting genes in ovarian cancer through integrated copy number and expression analysis. PLoS One 5: e9983.
10. Slavin TP, Feng T, Schnell A, Zhu X, Elston RC (2011) Two-marker association tests yield new disease associations for coronary artery disease and hypertension. Hum Genet 130: 725–733.
11. Comabella M, Craig DW, Morcillo-Suarez C, Rio J, Navarro A, et al. (2009) Genome-wide scan of 500,000 single-nucleotide polymorphisms among responders and nonresponders to interferon beta therapy in multiple sclerosis. Arch Neurol 66: 972–978.
12. Inoue N, Watanabe M, Yamada H, Takemura K, Hayashi F, et al. (2012) Associations Between Autoimmune Thyroid Disease Prognosis and Functional Polymorphisms of Susceptibility Genes, CTLA4, PTPN22, CD40, FCRL3, and ZFAT, Previously Revealed in Genome-wide Association Studies. J Clin Immunol 32: 1243–1252.
13. Carpenter AC, Bosselut R (2010) Decision checkpoints in the thymus. Nat Immunol 11: 666–673.
14. Starr TK, Jameson SC, Hogquist KA (2003) Positive and negative selection of T cells. Annu Rev Immunol 21: 139–176.
15. Goldrath AW, Bevan MJ (1999) Selecting and maintaining a diverse T-cell repertoire. Nature 402: 255–262.
16. Germain RN (2002) T-cell development and the CD4–CD8 lineage decision. Nat Rev Immunol 2: 309–322.
17. Werlen G, Palmer E (2002) The T-cell receptor signalosome: a dynamic structure with expanding complexity. Curr Opin Immunol 14: 299–305.
18. Fischer AM, Katayama CD, Pages G, Pouyssegur J, Hedrick SM (2005) The role of erk1 and erk2 in multiple stages of T cell development. Immunity 23: 431–443.
19. McNeil LK, Starr TK, Hogquist KA (2005) A requirement for sustained ERK signaling during thymocyte positive selection in vivo. Proc Natl Acad Sci U S A 102: 13574–13579.
20. Bettini ML, Kersh GJ (2007) MAP kinase phosphatase activity sets the threshold for thymocyte positive selection. Proc Natl Acad Sci U S A 104: 16257–16262.
21. Shao H, Kono DH, Chen LY, Rubin EM, Kaye J (1997) Induction of the early growth response (Egr) family of transcription factors during thymic selection. J Exp Med 185: 731–744.
22. Basson MA, Wilson TJ, Legname GA, Sarner N, Tomlinson PD, et al. (2000) Early growth response (Egr) −1 gene induction in the thymus in response to TCR ligation during early steps in positive selection is not required for CD8 lineage commitment. J Immunol 165: 2444–2450.
23. Schnell FJ, Kersh GJ (2005) Control of recent thymic emigrant survival by positive selection signals and early growth response gene 1. J Immunol 175(4): 2270–2277.
24. Bettini M, Xi H, Milbrandt J, Kersh GJ (2002) Thymocyte development in early growth response gene 1-deficient mice. J Immunol 169: 1713–1720.
25. Lawson VJ, Weston K, Maurice D (2010) Early growth response 2 regulates the survival of thymocytes during positive selection. Eur J Immunol 40: 232–241.
26. Xi H, Kersh GJ (2004) Early growth response gene 3 regulates thymocyte proliferation during the transition from CD4−CD8− to CD4+CD8+. J Immunol 172: 964–971.
27. Marrack P, Kappler J (2004) Control of T cell viability. Annu Rev Immunol 22: 765–787.
28. Hamrouni A, Olsson A, Wiegers GJ, Villunger A (2007) Impact of cellular lifespan on the T cell receptor repertoire. Eur J Immunol 37: 1978–1985.

29. Michie AM, Zuniga-Pflucker JC (2002) Regulation of thymocyte differentiation: pre-TCR signals and beta-selection. Semin Immunol 14: 311–323.
30. Taghon T, Yui MA, Pant R, Diamond RA, Rothenberg EV (2006) Developmental and molecular characterization of emerging beta- and gammadelta-selected pre-T cells in the adult mouse thymus. Immunity 24: 53–64.
31. Miyazaki M, Kawamoto H, Kato Y, Itoi M, Miyazaki K, et al. (2005) Polycomb group gene mel−18 regulates early T progenitor expansion by maintaining the expression of Hes−1, a target of the Notch pathway. J Immunol 174: 2507–2516.
32. Falahati R, Leitenberg D (2008) Selective regulation of TCR signaling pathways by the CD45 protein tyrosine phosphatase during thymocyte development. J Immunol 181: 6082–6091.
33. Stojakovic M, Salazar-Fontana LI, Tatari-Calderone Z, Badovinac VP, Santori FR, et al. (2008) Adaptable TCR avidity thresholds for negative selection. J Immunol 181: 6770–6778.
34. Hogquist KA, Jameson SC, Heath WR, Howard JL, Bevan MJ, et al. (1994) T cell receptor antagonist peptides induce positive selection. Cell 76: 17–27.
35. Barnden MJ, Allison J, Heath WR, Carbone FR (1998) Defective TCR expression in transgenic mice constructed using cDNA-based alpha- and beta-chain genes under the control of heterologous regulatory elements. Immunol Cell Biol 76: 34–40.
36. Palacios EH, Weiss A (2004) Function of the Src-family kinases, Lck and Fyn, in T-cell development and activation. Oncogene 23: 7990–8000.
37. DeSilva DR, Jones EA, Favata MF, Jaffee BD, Magolda RL, et al. (1998) Inhibition of mitogen-activated protein kinase kinase blocks T cell proliferation but does not induce or prevent anergy. J Immunol 160: 4175–4181.
38. Lauritsen JP, Kurella S, Lee SY, Lefebvre JM, Rhodes M, et al. (2008) Egr2 is required for Bcl−2 induction during positive selection. J Immunol 181: 7778–7785.
39. Baniyash M (2004) TCR zeta-chain downregulation: curtailing an excessive inflammatory immune response. Nat Rev Immunol 4: 675–687.
40. Lee KM, Chuang E, Griffin M, Khattri R, Hong DK, et al. (1998) Molecular basis of T cell inactivation by CTLA−4. Science 282: 2263–2266.
41. Myers MD, Sosinowski T, Dragone LL, White C, Band H, et al. (2006) Src-like adaptor protein regulates TCR expression on thymocytes by linking the ubiquitin ligase c-Cbl to the TCR complex. Nat Immunol 7: 57–66.
42. Anand PK, Malireddi RK, Lukens JR, Vogel P, Bertin J, et al. (2012) NLRP6 negatively regulates innate immunity and host defence against bacterial pathogens. Nature 488: 389–393.

OPEN ACCESS Freely available online

PLOS ONE

Differential Function of Themis CABIT Domains during T Cell Development

Toshiyuki Okada[1☯], Takeshi Nitta[1☯], Kentaro Kaji[1], Akiko Takashima[1], Hiroyo Oda[1], Norimasa Tamehiro[1], Motohito Goto[2], Tadashi Okamura[2,3], Michael S. Patrick[1], Harumi Suzuki[1]*

1 Department of Immunology and Pathology, Research Institute, National Center for Global Health and Medicine, Ichikawa-shi, Chiba, Japan, **2** Department of Laboratory Animal Medicine, Research Institute, National Center for Global Health and Medicine, Shinjuku, Tokyo, Japan, **3** Department of Infectious Diseases, Research Institute, National Center for Global Health and Medicine, Shinjuku, Tokyo, Japan

Abstract

Themis (also named Gasp) is a newly identified Grb2-binding protein that is essential for thymocyte positive selection. Despite the possible involvement of Themis in TCR-mediated signal transduction, its function remains unresolved and controversial. Themis contains two functionally uncharacterized regions called CABIT (cysteine-containing, all-β in Themis) domains, a nuclear localization signal (NLS), and a proline-rich sequence (PRS). To elucidate the role of these motifs in Themis's function in vivo, we established a series of mutant Themis transgenic mice on a Themis$^{-/-}$ background. Deletion of the highly conserved Core motif of CABIT1 or CABIT2 (Core1 or Core2, respectively), the NLS, or the PRS abolished Grb2-association, as well as TCR-dependent tyrosine-phosphorylation and the ability to induce positive selection in the thymus. The NLS and Core1 motifs were required for the nuclear localization of Themis, whereas Core2 and PRS were not. Furthermore, expression of ΔCore1- but not ΔCore2-Themis conferred dominant negative-type inhibition on T cell development. Collectively, our current results indicate that PRS, NLS, CABIT1, and CABIT2 are all required for positive selection, and that each of the CABIT domains exerts distinct functions during positive selection.

Citation: Okada T, Nitta T, Kaji K, Takashima A, Oda H, et al. (2014) Differential Function of Themis CABIT Domains during T Cell Development. PLoS ONE 9(2): e89115. doi:10.1371/journal.pone.0089115

Editor: Jon C. D. Houtman, University of Iowa, United States of America

Received October 18, 2013; **Accepted** January 15, 2014; **Published** February 21, 2014

Funding: This work was supported by JSPS Grant-in-Aid for Scientific Research (B) 22390098, and grant for National Center for Global Health and Medicine (21-111, 22-303). The funders had no role in study design, data collection and analysis, decision to publish, or preparation of the manuscript.

Competing Interests: The authors have declared that no competing interests exist.

* E-mail: hsuzuki@ri.ncgm.go.jp

☯ These authors contributed equally to this work.

Introduction

T cells develop through positive and negative selection in the thymus to become either class II MHC-restricted helper $CD4^+CD8^-$ [CD4-single positive (CD4SP)] or class I MHC-restricted cytotoxic $CD4^-CD8^+$ (CD8SP) cells [1]. However, the molecular mechanisms of TCR-mediated selection in developing T cells are not yet fully understood.

Themis (thymocyte-expressed molecule involved in selection) was identified as a novel mandatory factor for positive selection by five independent groups in 2009 [2-3-4-5-6]. We identified Themis (initially named Gasp) from a set of uncharacterized genes whose expression was restricted to the thymus [2]. Themis knockout mice exhibited significantly reduced numbers of CD4SP and CD8SP T cells both in the thymus and periphery [2-3-4-5-6]. Inhibitory effects of Themis deficiency on negative selection and T cell activation were controversial among the reports [2-3-4-5], nevertheless, they were much slighter than that for positive selection. Thus, Themis is a unique molecule that is essential for positive selection, but not for negative selection. Expression of Themis was significantly lower in regulatory T cells (Tregs) compared to conventional T cells [7], however, study of a natural mutant rat revealed the importance of Themis on the function of Tregs [8]. Since Themis-deficient mice did not exhibit inflammatory bowel disease or autoimmune diseases observed in Treg-deficient mice, functional requirements for Themis in Tregs could be different between rat and mouse.

Themis is constitutively associated with Grb2 and is tyrosine-phosphorylated by Lck and ZAP-70 upon TCR stimulation [5-9-10]. Some groups reported constitutive association of Themis with Vav1 [9], Itk, and PLC-γ1 [5-10-11]. Furthermore, we and other groups (Fig. S3) demonstrated association of Themis with PLC-γ1, LAT, and SLP76 [5-9-10-11] upon TCR-stimulation, indicating that Themis would be a component of the SLP76-LAT signalosome. From these results, Themis is likely to be involved in TCR-mediated signal transduction. Accordingly, TCR-dependent activation of ERK and NFAT, as well as production of IL-2 was significantly reduced in Themis knockdown Jurkat cells [10]. In the Themis-knockout mice, however, results were different. We and other groups observed unaltered activation of ERK and calcium influx in Themis deficient immature DP thymocyte upon anti-CD3 antibody stimulation [2-3-4], although one group reported impaired activation of these signaling events [5]. Moreover, recent study showed that TCR-dependent activation of ERK, p38 and Vav1 were reduced in Themis deficient CD4SP and CD8SP thymocytes [9]. After all, results were not consistent between different groups possibly because of different experimental systems, and therefore no consensus has been reached about the effect of Themis on TCR-mediated signal transduction.

Themis contains two novel cysteine-based CABIT (cysteine-containing, all beta in Themis) domains [4], a bipartite type nuclear localization sequence (NLS), and a proline-rich sequence (PRS). The CABIT domain is a newly designated domain structure conserved among metazoans, and it could adopt an all-beta-strand structure with at least 12 strands, which suggests either an extended beta-sandwich-like fold or a dyad of six-stranded beta-barrel units [4]. In mammals, the CABIT domains are conserved among three Themis family proteins (Themis/Themis1, ICB1/Themis2 and 9130404H23Rik/Themis3) harboring two tandemly-repeated CABIT domains (CABIT1 and CABIT2) and two Fam59 proteins (Fam59a and b) containing one CABIT domain [4]. Although a number of proteins containing CABIT domains have been identified, their function is totally unknown. Therefore, elucidation of the function of CABIT domains has long been awaited.

In order to reveal the function of Themis in positive selection, we investigated the function of each structural domain and motif in Themis. In the present study, we generated a series of transgenic (Tg) mice expressing mutant Themis proteins lacking each domain on a Themis$^{-/-}$ background. Deleted motifs were the PRS and the highly conserved cysteine-containing Core motif of the CABIT1 or CABIT2 domain (Core1 and Core2, respectively). We found that the PRS, Core1, and Core2 motifs were all required for Grb2-binding and TCR-dependent tyrosine-phosphorylation, as well as for positive selection in the thymus. Interestingly, the Core1 and NLS motifs were required for nuclear localization of Themis, whereas Core2 and PRS were not. Furthermore, Core1- but not Core2-deleted mutant exhibited a dominant negative inhibitory effect on T cell development even in the presence of wild-type Themis. These results indicate that each structural motif in Themis exerts an essential but distinct role in T cell development, and that the two CABIT domains in Themis have distinct functions.

Materials and Methods

Mice

Themis$^{-/-}$ mice have been previously described [2]. For generation of Themis transgenic mice, PCR-cloned cDNA fragments encoding WT or ΔPRS,ΔNLS, ΔCore1, ΔCore2, or CAB2-1 mutants of Themis were inserted into the hCD2-VA vector [12]. The transgenes were purified and microinjected into the pronuclei of fertilized eggs from mixed background mice [BDF1 (SLC)×Themis$^{-/-}$ mice on a C57BL/6 background] using standard procedures. The embryos were transferred to the oviducts of pseudopregnant ICR female mice. Previous studies have shown the human CD2 promoter/enhancer directs the expression of transgenes in mice to the T cell lineage [12]. The ΔPRS, ΔCore1, and ΔCore2-Tg mice used in the study were homozygous for transgene (ΔPRS-Tg$^{+/+}$, ΔCore1-Tg$^{+/+}$, ΔCore2-Tg$^{+/+}$) with the exception of ΔCore1-Tg$^{+/-}$ in the Fig. S4. Instead, the ΔNLS-, WT, and CAB2-1-Tg mice were heterozygous for transgene (ΔNLS-Tg$^{+/-}$, WT-Tg$^{+/-}$, CAB2-1-Tg$^{+/-}$). All mice were housed under specific pathogen-free conditions. All animal experiments were approved by the Animal Care and Use Committee of the National Center for Global Health and Medicine (NCGM) Research Institute, and conducted in accordance with institutional procedures.

TCR Stimulation

Thymocytes were pre-treated with biotin-conjugated anti-CD3ε (145-2C11, Biolegend) and anti-CD4 (RM4-4, eBioscience) antibodies (10 μg/mL each) at 4°C for 30 min. Cells were then washed, resuspended in RPMI-1640 complete medium, and stimulated with streptavidin (BECKMAN COULTER, 10 μg/mL) at 37°C for the indicated times. Ice-cold PBS or paraformaldehyde (final concentration of 2%) was added to stop stimulation.

Immunoprecipitations and Western Blot Analysis

Cells were lysed with lysis buffer (50 mM Tris-HCl [pH7.5], 150 mM NaCl, 10 mM $MgCl_2$, 0.5% Nonidet P-40) containing protease and phosphatase inhibitor cocktail (Thermo Scientific)). Cell lysates were immunoprecipitated with antibodies conjugated to protein G-sepharose beads (GE). Antibodies used for immunoprecipitation were anti-Themis pAb (06-1328, Millipore) and anti-Themis mAb 2E7. 2E7 is a rat monoclonal antibody produced against recombinant full-length Themis from mice [2]. Antibodies used for western blotting are as follows: anti-Grb2 (MS-20-3, MBL), anti-phospho-tyrosine 4G10 (05-321, Millipore), anti-PLCγ-1 (2822, Cell Signaling), anti-LAT (9166, Cell Signaling), anti-CRK (610035, BD), anti-PARP (ab6079, Abcam), anti-SOS1/2 (SC-259, SantaCruz), and anti-HA (3F10, Roche). Horseradish peroxidase-conjugated anti-IgG secondary antibodies against rabbit, rat, or mouse IgG (GE) were used with Lumigo substrate (Cell signaling).

Flow Cytometry

For cell-surface staining, the following Abs were used: anti-CD25 (PC61), anti-CD62L (MEL-14), anti-CD4 (RM4-5 and GK1.5), anti-CD8α (5H10-1 and 53-6.7), anti-Foxp3 (FJK-16a), anti-TCRβ (H57-597), anti-CD69 (H1.2F3), anti-CD44 (IM7) Abs. All antibodies were purchased from eBioscience or Biolegend. To examine ERK phosphorylation, cells were fixed and permeabilized with 90% methanol and stained with anti-phospho-ERK (197G2, Cell Signaling) Ab. Foxp3 staining was performed using the FOXP3 staining kit (00-5523-00, eBioscience) according to the manufacturer's protocol. Cells were analyzed using a FACS CantoII (Becton Dickinson), and the data were analyzed using FlowJo software (Tree Star).

Subcellular Protein Fractionation

Nuclear and cytoplasmic fractions were isolated from total thymocytes or sorted DP thymocytes using the Subcellular Protein Fractionation Kit (Pierce) following the manufacturer's protocol.

Immunofluorescence Confocal Microscopy

Thymocytes were fixed with 2% paraformaldehyde and permeabilized with 0.1% saponin, and stained with anti-Themis antibody (06-1328, Millipore) or isotype control antibody, followed by staining with Alexa-fluor 647-conjugated anti-rabbit IgG (A21246, Molecular Probes, 5 μg/mL) and DAPI (0.2 μg/mL). Images were collected with an Olympus FV-1000 multitracking laser scanning confocal microscope (Olympus Japan) with a 100 × oil objective (NA 1.4), giving a resolution of 0.9 μm in the X, Y – plane.

Statistical Analysis

All data are represented as means ± SEM. Flow cytometric data were analyzed using the Unpaired T test (GraphPad Prism version 5.0). Asterisks in all figures are as follows: *P<0.05; **P<0.01; ***P<0.001. N.S.; not significant.

Results

Establishment of Mutant Themis Transgenic Mouse Lines

To determine whether the structural motifs of Themis contribute to its function, we generated a series of transgenic mice expressing mutant Themis proteins lacking each domain (Fig. 1A, Fig. S1). The Themis mutants used in the present study were as follows: ΔPRS (lacking the PRS: aa 555-563), ΔNLS (lacking the NLS: aa 345-349), ΔCore1 (lacking the Core region of CABIT1 domain: aa 150-174), ΔCore2 (lacking the Core region of CABIT2 domain: aa 411-434), and CAB2-1 (swapping entire region of CABIT1 [aa 1-261] and CABIT2 [aa 262-521]). These mutant proteins were expressed under the control of the human CD2 promoter [12]. Each Tg line was then bred with Themis$^{-/-}$ mice to replace endogenous wild-type Themis with each mutant Themis. As shown by Western blotting analysis in Fig. 1B, expression of mutant Themis protein in each Tg line was almost comparable to the endogenous Themis$^{+/+}$ level, although expression of ΔCore2 and CAB2-1 were more comparable to Themis$^{+/-}$ level. As has been reported [9], introduction of a CD2-driven wild-type Themis transgene into Themis$^{-/-}$ mice successfully recovered defective positive selection in the knockout (Fig. 2A), proving that this transgenic approach is useful to evaluate the function of Themis mutant proteins *in vivo*.

The PRS, NLS, Core1, and Core2 Motifs in Themis are all Required for Positive Selection

First, we analyzed positive selection using these mutant mice. Themis$^{-/-}$ mice showed a marked reduction of CD4SP and CD8SP thymocytes and splenocytes (Fig. 2A) as has been reported [2-3-4-5-6]. Although the transgenic expression of WT Themis completely restored T cell development in Themis$^{-/-}$ mice (Fig. 2A), none of the mutants (ΔPRS, ΔNLS, ΔCore1, ΔCore2, CAB2-1) could restore positive selection. In the thymus, generation of CD4-SP in these mutants was the same or even less than the knockout (Fig. 2A–B, Fig. S2A) with the exception of the NLS mutant which showed some recovery of CD4-SP thymocytes (Fig. 2A–B). In the ΔPRS mutant, peripheral CD4SP cells were significantly recovered despite the defective positive selection in the thymus, suggesting that PRS might not be critical in peripheral expansion and survival of mature T cells. The NLS mutant also showed some recovery of CD4-SP in the periphery, possibly because of the milder defect of positive selection in the thymus. Interestingly, ΔCore1 mutant mice exhibited a severer inhibition of T cell development than the Themis deficient mice. These mice also showed decreased numbers of thymic DP, which was not seen in Themis knockout mice. Also, post-selected (CD69^{+}, TCR^{hi}) DP thymocytes were significantly fewer in the ΔCore1 mutant mice (Fig. S2C). Indeed, all of the T cell subsets in ΔCore1 Tg mice were fewer than the knockout (Fig. 2B). From these results, loss of the Core1 motif in Themis resulted in a severer phenotype than the loss of entire Themis. Finally, complete loss of positive selection in CAB2-1 mutant indicates that even the order of the two CABIT domains is critical for its function. Collectively, the PRS, NLS, Core1, and Core2 are all required for Themis's function, and each motif may have different roles.

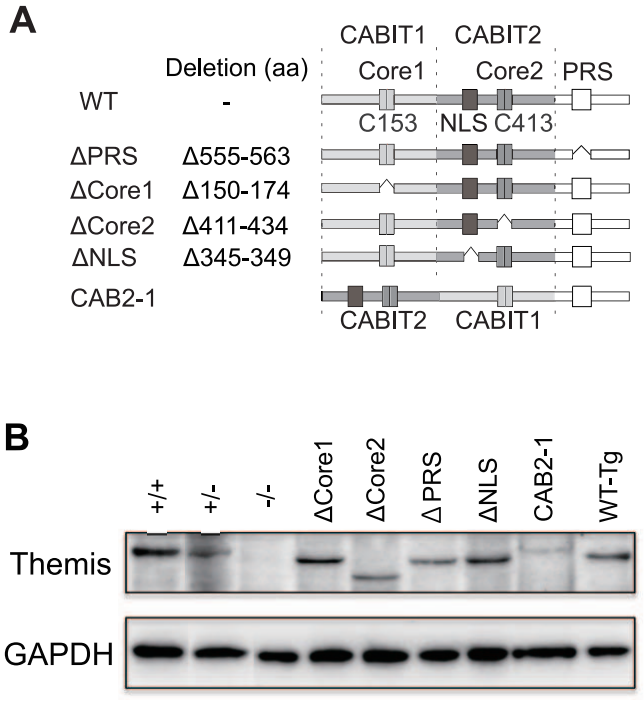

Figure 1. Generation of Themis$^{-/-}$ mice expressing mutant Themis proteins. (A) Schematic representation of the mutant Themis proteins. (B) Analysis of Themis protein expression by immunoblot using sorted CD69^{-} DP thymocytes from Themis$^{+/+}$, Themis$^{+/-}$, Themis$^{-/-}$ and Themis$^{-/-}$ mice expressing ΔPRS, ΔCore1, ΔCore2, ΔNLS, CAB2-1 mutant, or WT Themis. Data are representative of more than three independent experiments.
doi:10.1371/journal.pone.0089115.g001

PRS, NLS, CABIT1, and CABIT2 are Required for Tyrosine-phosphorylation and Grb2-association

We and other groups previously reported that Themis constitutively associates with Grb2 [2,3,9-11], and is tyrosine-phosphorylated upon TCR stimulation [5,9-11]. We then investigated whether the deletion of each motif affects Grb2-association and tyrosine-phosphorylation. We observed that endogenous wild-type Themis constitutively associated with Grb2 in thymocytes, and was tyrosine-phosphorylated upon stimulation with anti-CD3 plus anti-CD4 antibodies (Fig. 3A) as previously reported [2-5,9-11]. In addition, we observed stimulation-dependent association of Themis with PLC-γ1 and SOS (Fig. S3A), suggesting a possible involvement of Themis as a component of the SLP76/LAT-signalosome complex [11]. As shown in Fig. 3A, we could successfully immunoprecipitate ΔPRS, ΔNLS, ΔCore1, ΔCore2, and CAB2-1 Themis mutant proteins, but all of these mutant Themis proteins lost constitutive association with Grb2. Additionally, all five mutants also lost tyrosine-phosphorylation upon TCR stimulation (Fig. 3A). These results indicate that the PRS, NLS, Core1, and Core2 motif, as well as order of the two CABIT domains are all critical for Grb2-association and tyrosine-phosphorylation of Themis.

Because a previous *in vitro* study reported that Themis binds to Grb2 via its PRS motif [11], inability of ΔNLS, ΔCore1, ΔCore2 and CAB2-1 mutants to associate with Grb2 was quite surprising. Therefore, we decided to reinvestigate the biochemical basis of the Themis-Grb2 interaction in thymocytes. We utilized our monoclonal antibody (mAb) against Themis (clone 2E7) [2], which recognizes an epitope around the PRS (aa 555-563) (Fig. 3B). We found that the 2E7 mAb binds only to Grb2-unbound Themis, but not to Grb2-bound Themis by sequential immunoprecipitation experiments (Fig. 3C). These results strongly indicate that 2E7 mAb and Grb2 compete for binding to the PRS, supporting direct association of Grb2 with the PRS of Themis in thymocytes.

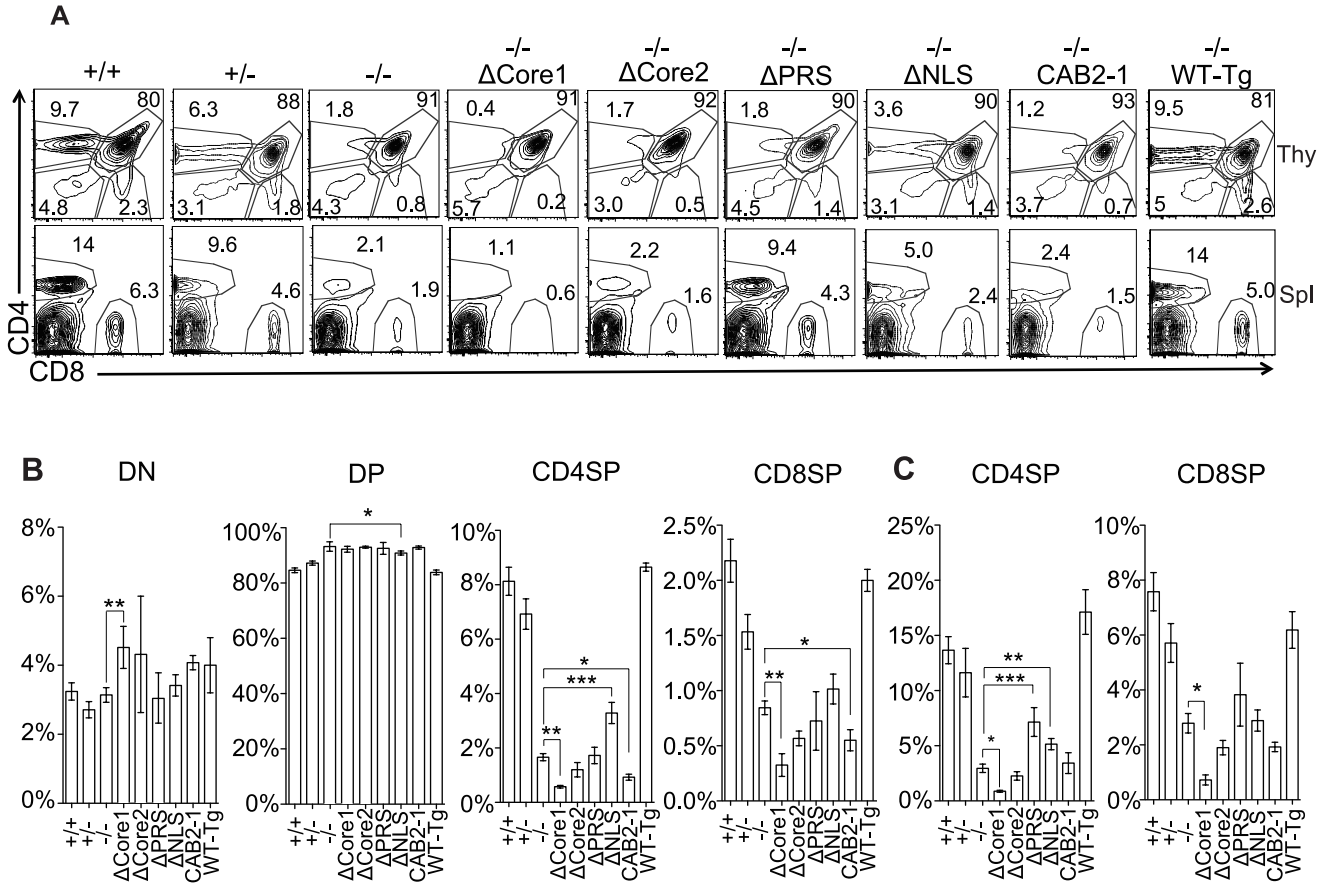

Figure 2. Expression of the Themis mutants failed to restore positive selection in Themis$^{-/-}$ mice. (A) CD4 and CD8 expression profiles of thymocytes or splenocytes from Themis mutant mice. Numbers in plots show the frequency of cells in the indicated area. Proportion (%) of indicated subsets of (B) thymocytes and (C) splenocytes (mean ± SEM). (A-C) Data are representative of more than three independent experiments. Only significant differences against −/− mice are noted in the graphs. *p<0.05, **p<0.01, ***p<0.001.
doi:10.1371/journal.pone.0089115.g002

The Core1 but not Core2 Motif is Required for Nuclear Localization

Although initial experiments using a GFP-fusion protein of Themis exhibited cytosolic localization of Themis protein [2-4], Western-blotting results by subcellular fractionation proved that endogenous Themis exists in the nucleus as well as the cytosol [3-9]. In fact, we also confirmed the existence of endogenous Themis protein in nuclear fractions by Western blotting (Fig. 4A). Furthermore, existence of Themis in the nucleus was also confirmed by immunostaining analysis by confocal fluorescence microscopy. As shown in Fig. 4B, Themis was visualized in cytosol, as well as in the nucleus as punctate staining. Staining of DNA and Themis appeared mutually exclusive, suggesting that Themis exists unassociated with DNA in the nucleus. We next investigated nuclear localization of each mutant Themis protein in thymocytes by subcellular fractionation. As shown in Fig. 4C-D, ΔPRS and ΔCore2 mutant Themis successfully translocated to the nucleus similar to wild-type Themis, whereas ΔCore1 and ΔNLS mutant existed only in the cytosol (Fig. 4C-D). Although the importance of the NLS motif on nuclear localization of Themis protein has been reported by another group [9], we further showed the Core1 motif to be essential for nuclear translocation of Themis. Furthermore, the order of the two CABIT domains was also critical for the translocation. From these results, we conclude that not only NLS but also the Core motif in the CABIT-1 domain are important for nuclear translocation of Themis.

Dominant Negative Inhibitory Effect of ΔCore1 Mutant on T Cell Development

We observed that ΔCore1 mutant Tg mice in Themis$^{-/-}$ background showed severer and distinct defects on T cell development when compared to Themis$^{-/-}$ mice (Fig. 2A). These results indicate that ΔCore1 mutant protein could affect T cell development in a dominant negative fashion. To confirm this possibility, we investigated the phenotype of ΔCore1 Tg mice on a Themis$^{+/+}$ background. Indeed, positive selection of both CD4SP and CD8SP thymocytes was significantly decreased in ΔCore1-Tg Themis$^{+/+}$ mice, whereas ΔCore2-Tg Themis$^{+/+}$ mice did not exhibit any significant change (Fig. 5A). Absolute numbers of DP thymocytes in ΔCore1-Tg Themis$^{+/+}$ were also reduced, which is totally different from the phenotype of Themis deficiency. In addition, numbers of peripheral CD4SP and CD8SP cells were severely reduced in ΔCore1-Tg mice. In ΔCore1-Tg Themis$^{+/+}$ mice we also observed a strong reduction of the earliest post-selected DP (CD69^{hi} TCR^{hi}) thymocytes, whereas the reduction was slight in the ΔCore2-Tg Themis$^{+/+}$ mice (Fig. 5B). Expression of CD25 and CD44 on DP thymocytes was somehow increased in ΔCore1-Tg, but not in ΔCore2-Tg Themis$^{+/+}$ mice (Fig. 5C). In the periphery of ΔCore1-Tg Themis$^{+/+}$ mice, memory CD4SP and CD8SP cells (CD44^{hi} CD62L^{lo}) were strongly increased with a concomitant decrease of naive populations (CD44^{lo} CD62L^{hi}), possibly because of homeostatic expansion in lymphopenic mice (Fig. 5D). Again, this increase of the memory population was

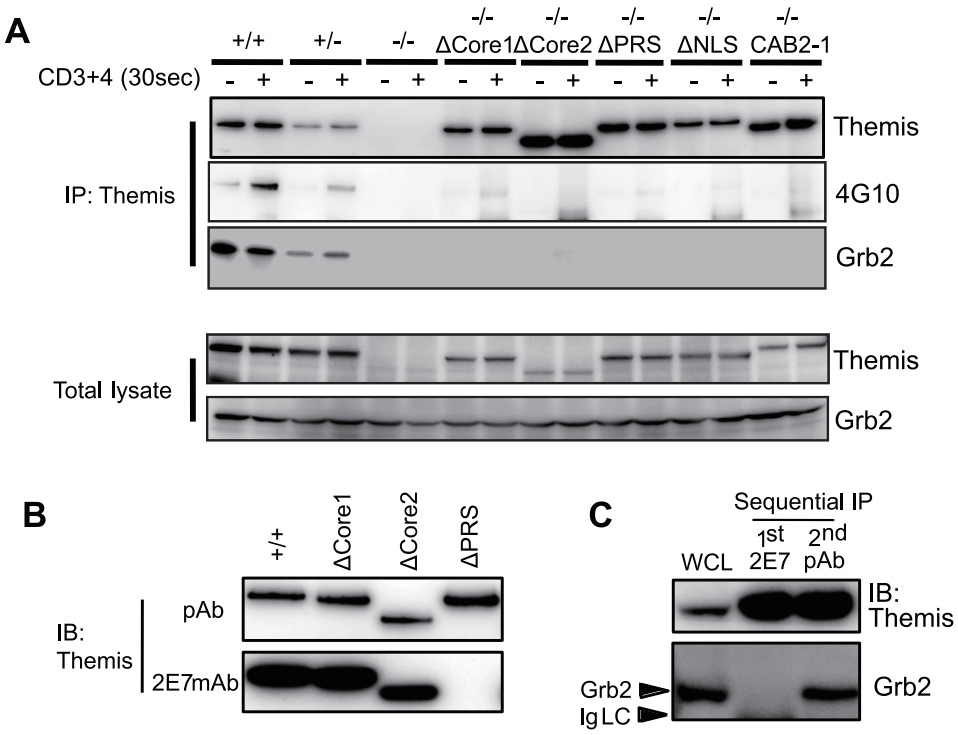

Figure 3. Themis mutants lack tyrosine-phosphorylation and Grb2-association. (A) Analysis of tyrosine-phosphorylation and protein interactions of Themis mutants. Thymocytes from the indicated mutant mice were stimulated with anti-CD3 plus anti-CD4 antibodies. Proteins were immunoprecipitated (IP) with anti-Themis antibody and analyzed by immunoblot (IB) with the indicated antibodies. Data are representative of four independent experiments. (B) Anti-Themis monoclonal antibody (mAb) 2E7 binds to the PRS motif. Immunoprecipitated Themis proteins from Themis$^{+/+}$, Themis$^{-/-}$ ΔCore1, Themis$^{-/-}$ ΔCore2 and Themis$^{-/-}$ ΔPRS thymocytes were immunoblotted with anti-Themis mAb 2E7. Data are representative of three independent experiments. (C) Cell lysates from Themis$^{+/+}$ thymocytes were sequentially immunoprecipitated with 2E7 and anti-Themis polyclonal antibody (pAb). Grb2 was co-precipitated with anti-Themis pAb but not with 2E7. Data are representative of three independent experiments.
doi:10.1371/journal.pone.0089115.g003

observed only in ΔCore1-Tg, but not in ΔCore2-Tg Themis$^{+/+}$ mice. Since ΔCore1-Tg Themis$^{+/+}$ mice showed a strong defect in positive selection, we investigated TCR-dependent activation of ERK [13], which is critical in the process. As shown in Fig. 5E, anti-CD3 plus anti-CD4 mAb stimulated phosphorylation of ERK was strongly inhibited in the presence of ΔCore1 mutant Themis but not of ΔCore2 mutant. Therefore, decreased positive selection in ΔCore1-Tg mice could partly be due to the impaired ERK activation. We also found that the absolute number of CD25^{+}Foxp3^{+} natural regulatory T cells (nTreg) in the thymus was significantly reduced in ΔCore1-Tg, but not in ΔCore2-Tg Themis$^{+/+}$ mice (Fig. 5F). Differentiation of NKT and γδ-T cells in Themis$^{+/+}$ ΔCore1 mice was not changed (data not shown). Collectively, expression of Core1-deleted Themis in immature thymocytes caused dominant-negative type inhibition of T cell development, possibly by interfering with signaling related to ERK activation. All of these analyses were carried out using transgene homozygous (ΔCore1-Tg$^{+/+}$ or ΔCore2-Tg$^{+/+}$) mice. Because expression levels of mutant protein in ΔCore2-Tg$^{+/+}$ were significantly less than that of ΔCore1-Tg$^{+/+}$ mice, one can assume that the absence of dominant negative effects in ΔCore2-Tg mice was simply due to the fewer expression of less ΔCore2 mutant protein. Therefore, we compared transgene heterozygous (ΔCore1-Tg$^{+/-}$) mice with homozygous (ΔCore2-Tg$^{+/+}$) mice. As shown in Fig. S4A, protein expression level of mutant Themis protein in ΔCore1-Tg$^{+/-}$ mice and ΔCore2-Tg$^{+/+}$ mice were the same, which were equivalent with that of Themis$^{+/-}$ mice. Although expression of the two mutant proteins were the same level, only ΔCore1-Tg showed dominant negative effects (Fig. S4B-C), proving that the effect is specific to the ΔCore1 mutant protein. Since the dominant negative inhibitory effects were only observed in ΔCore1-Tg but not in ΔCore2-Tg, our current results clearly indicated distinct functions for CABIT1 and CABIT2 domains.

Discussion

Themis contains an NLS, PRS, and two CABIT domains. The CABIT domain, which was identified by Schwartz's group, is conserved through protozoa and is predicted to form either an extended beta-sandwich-like fold or a dyad of 6-strand beta-barrel structures [4]. Themis family proteins (Themis, Themis2, and Themis3) contain two CABIT domains and a PRS. A recent report demonstrated that Themis and Themis2 were functionally interchangeable in terms of T cell development [9], indicating the important function of CABIT domains. Therefore, in the present study, we focused on the function of CABIT domains, especially on differences in the two CABIT domains in Themis.

To elucidate the involvement of each domain/motif in Themis on its function in positive selection, we established several mutant Themis Tg lines. Because Themis$^{+/-}$ mice showed an intermediate effect on positive selection between Themis$^{+/+}$ and Themis$^{-/-}$ mice [2], it is obvious that the expression level of Themis protein in thymocytes critically affects the result of positive selection. Therefore, the expression level of mutant protein in these Tg mice is important for evaluating their function. We

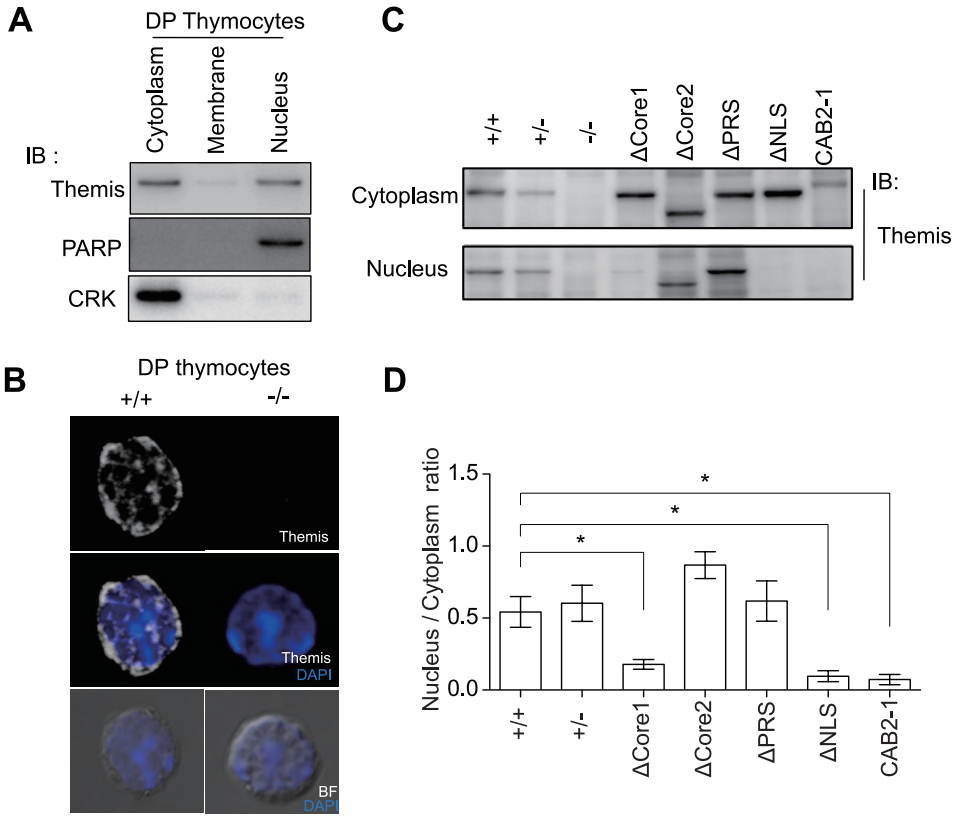

Figure 4. The CABIT1 domain of Themis is important for nuclear localization. (A) DP-thymocytes from Themis$^{+/+}$ mice were fractionated into cytoplasm, membrane and nuclear fractions and immunoblotted with indicated Abs. The CRK and PARP proteins were used as purity controls for the cytoplasmic and nuclear fractions, respectively. Data are representative of more than four independent experiments. (B) Representative micrograph showing localization of Themis (white) in cytoplasm and nucleus stained with DAPI (blue), together with BF (bright field). Data are representative of three independent experiments. (C) Localization of Themis mutants was analyzed by Western blot in cytoplasmic and nuclear extracts. Thymocytes from Themis mutant mice were fractionated into the cytoplasm and nucleus. (D) Bar graph shows that the nuclear/cytoplasmic Themis protein ratio compared with Themis$^{+/+}$ mice. Data are representative of more than three independent experiments. Significant differences are noted in the graphs. *$p<0.05$.
doi:10.1371/journal.pone.0089115.g004

screened a large number of founder lines of each mutant transgene and managed to establish lines with comparable protein expression (Fig. 1B).

Very recently, the PRS motif was reported to be important for Grb2-association, tyrosine-phosphorylation, and positive selection, using irradiation-mediated chimeric mice reconstituted with retrovirally transduced bone marrow cells [11]. It would be difficult to evaluate the expression level of mutant Themis protein in reconstituted thymocytes, however, our present results using ΔPRS-Tg mice with equivalent protein expression with endogenous Themis (Fig. 1B) strongly supported their observations. Despite strong inhibition of positive selection in the thymus of ΔPRS mice, the number of CD4SP in the periphery was significantly increased compared to Themis$^{-/-}$ mice, suggesting that the PRS motif in Themis is critical in positive selection in the thymus, but may not be important in peripheral survival and maintenance of mature T cells.

We firstly demonstrated that the consensus motif of CABIT2 domain (Core2) was crucial for positive selection. Furthermore, deletion of the Core1 motif resulted in a much severer inhibition of T cell development than seen in Themis$^{-/-}$ mice. Therefore, we next investigated the phenotype of ΔCore1- and ΔCore2-Tgs on a wild-type background. The ΔCore1-Tg mice in Themis$^{+/+}$ background showed decreased numbers of DP thymocytes, strong inhibition of CD8SP thymocyte development, reduced numbers of thymic nTregs, and an increased memory population (CD44^{hi} CD62L^{lo}) of peripheral mature T cells. The DP thymocytes from ΔCore1-Tg showed decreased ERK activation upon TCR stimulation. These phenotypes were not observed in Themis$^{-/-}$ mice, suggesting that the ΔCore1 mutant inhibits T cell development in a Themis-independent manner. Instead, the ΔCore1 mutant may perturb the function of unidentified protein(s) that compensate the residual T cell development in Themis$^{-/-}$ mice. Lastly, and most importantly, the dominant negative inhibitory effects were not observed in either the ΔCore2-Tg mice or the wild-type Themis-Tg mice, indicating that the loss of the Core motif of either CABIT1 or CABIT2 domains induces qualitatively different effects. It is possibly explained by differential protein association with ΔCore1 and ΔCore2, or because of the lack of nuclear interaction of ΔCore1 with another protein. Because two independent lines of ΔCore1 Tg mice showed the identical phenotype, the phenotype must not be an artifact caused by the destruction of other genes by the insertion of Tg vector. The dominant negative effects were not due to higher protein expression of the ΔCore1 versus the ΔCore2 mutant, because heterozygous ΔCore1-Tg+/− mice, having equivalent protein expression with homozygous ΔCore2-Tg+/+ mice, also showed the same dominant negative phenotypes (Fig. S4A–C). Collectively, in the present study, we clearly demonstrated differential functions for CABIT1 and CABIT2 domains.

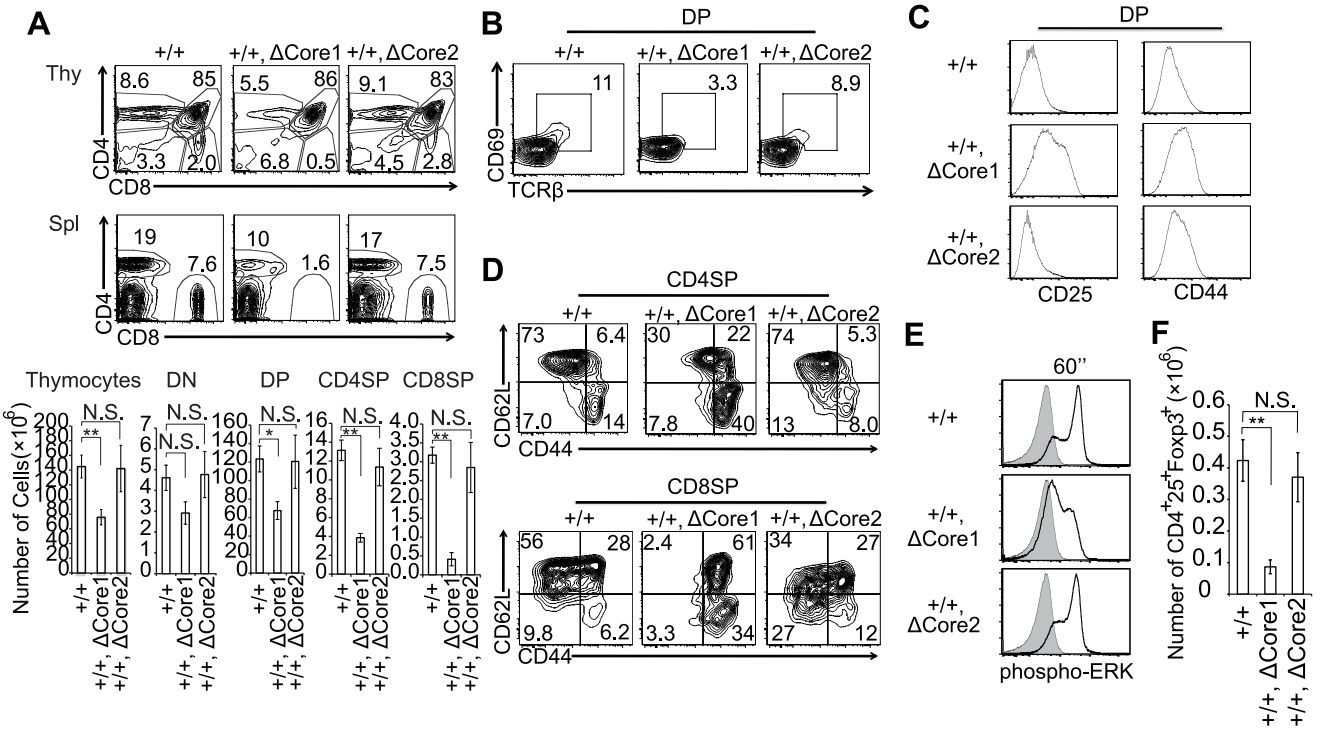

Figure 5. The CABIT1 and CABIT2 in Themis have different functions. (A) CD4 and CD8 profiles of thymocytes and splenocytes of Themis$^{+/+}$, Themis$^{+/+}$ ΔCore1, and Themis$^{+/+}$ ΔCore2 mice. Numbers in plots show the frequency of cells in the indicated area. Bar graphs show absolute number of total thymocytes and thymocyte subsets from Themis$^{+/+}$, Themis$^{+/+}$ ΔCore1, and Themis$^{+/+}$ ΔCore2 mice (mean ± SEM). Data are representative of four independent experiments. (B) Proportion of post-selected CD69^{+} TCR^{hi} cells in CD4^{+}CD8^{+} (DP) thymocytes. Data are representative of four independent experiments. (C) Surface expression of CD25 and CD44 on gated DP thymocytes. Data are representative of four independent experiments. (D) CD44 and CD62L profile of splenic CD4SP and CD8SP cells. Data are representative of four independent experiments. (E) Representative histogram overlays of phosphorylation of ERK. DP thymocytes were stimulated with anti-CD3 plus anti-CD4 Abs for 1min, then intracellular staining of phosphorylated-ERK antibody was performed (solid line). The shaded line is without stimulation. Data are representative of three independent experiments. (F) Absolute number of thymic CD4^{+}25^{+}Foxp3^{+} Treg cells (mean ± SEM). Data are representative of four independent experiments. Significant differences are noted in the graphs. *p<0.05, **p<0.01. N.S. = not significant.
doi:10.1371/journal.pone.0089115.g005

We demonstrated that Themis constitutively associates with Grb2 in thymocytes. Themis2 also associates with Grb2 [9], therefore Grb2-association must be an important feature of Themis family proteins. In the recent peptide inhibition study, the PRS motif of Themis was shown to directly interact with the C-terminal SH3 motif of Grb2 [11]. The result from immunoprecipitation experiments using our own anti-Themis monoclonal antibody (2E7) also supported direct binding of Grb2 to the PRS motif of Themis (Fig. 3B). As has been recently reported [9], we also observed defective association of the ΔPRS mutant Themis with Grb2 in thymocytes (Fig. 3A). More surprisingly, not only ΔPRS, but also all other mutants lost the ability to associate with Grb2 (Fig. 3A). These results suggest that the intra-molecular interaction of these domains is crucial to form the proper three-dimensional structure to associate with Grb2. Moreover, all of the five mutants in the present study lost not only Grb2 binding, but also tyrosine-phosphorylation. It should be noted that these five mutants also lost weak basal phosphorylation of the protein in unstimulated thymocytes (Fig. 3A).

From our sequential immunoprecipitation experiments, a half of Themis binds to Grb2 (Fig. 3C, Fig. S3C), and about one tenth of Grb2 binds to Themis (Fig. S3B). A recent study with T cell-specific Grb2-deficient mice revealed that Grb2 is critical for positive selection [14]. Although Grb2 has been reported to associate with several molecules (e.g. Sos, Shc, FAK) other than Themis [15-17], deficiency of Shc or FAK does not inhibit positive selection. Involvement of Sos in positive selection was also recently shown to be nonobligatory because Sos1/Sos2 DKO exhibited normal positive selection [18]. Therefore, Themis and Grb2 may be cooperatively required for positive selection. Further analysis of Themis/Grb2 DKO would clarify whether Themis and Grb2 are functionally complementary during positive selection.

We demonstrated that the PRS, NLS, Core1, and Core2 motifs were all required for Grb2-association, tyrosine-phosphorylation, and positive selection, whereas NLS and CABIT1 are required for nuclear translocation. The CABIT1 domain might be important for the interaction of Themis with nuclear transporter proteins. So far, the causal relationship between positive selection, Grb2-association, and tyrosine-phosphorylation is not yet understood, however, our results demonstrated that all of these are tightly correlated to one another. On the contrary, the current study demonstrated that positive selection and nuclear translocation of Themis are not directly correlated. As a matter of fact, it should be noted that deletion of the NLS motif exhibited the least effect on positive selection compared to the deletion of other motifs, indicating that nuclear translocation of Themis may be less important for positive selection.

Finally, this is the first report that describes the significance of the CABIT domain in cellular events. Furthermore, two CABIT domains exist in Themis are functionally different and not interchangeable. Although the structural basis for the function of CABIT domains remains to be elucidated, our study clearly

demonstrated that the two CABIT domains in Themis are pivotal and serve distinct roles in its function for driving T cell development.

Supporting Information

Figure S1 The amino acid sequence used for generation of mutant Themis transgenes.
(EPS)

Figure S2 Characterization of Themis transgenes lacking the Core1, Core2, PRS, or NLS motif in Themis$^{-/-}$ background mice. Bar graphs represent numbers of (**a**) thymocyte and (**b**) splenocyte subsets (mean ± SEM). (**c**) Proportion of post-selected CD69^{+}TCRβ^{hi} DP cells in each mutant. Results are representative of more than three independent experiments. Only significant differences in mutant-Tgs against −/− are noted in the graphs. *p<0.05, **p<0.01, ***p<0.0001.
(EPS)

Figure S3 Themis interacts with the LAT signalosome complex in thymocytes. (**a**) Thymocytes from Themis$^{+/+}$ and Themis$^{-/-}$ mice were stimulated with anti-CD3/anti-CD4/anti-CD8 Abs for indicated times at 37°C. Proteins were immunoprecipitated with anti-Themis pAb and analyzed by immunobloting with the indicated Abs. (**b**) Immunoprecipitates with anti-Themis Ab from Themis$^{+/+}$ thymocytes were immunoblotted with anti-Grb2. Bar graphs show the relative density of the immunoblots of Grb2 from total lysate, immunoprecipitates with anti-Themis (IP), and the supernatant after the immunoprecipitation (Sup). (**c**) Cell lysates from Themis$^{+/+}$ thymocytes were sequentially immunoprecipitated with 2E7 and anti-Themis Ab. Bar graphs show the relative density of the immunoblot Themis bands (mean ± SEM). Results are representation of three independent experiments. The relative densities are expressed as mean ± SEM.
(EPS)

Figure S4 Dominant-negative inhibitory effect observed in Themis$^{+/+}$ ΔCore1-Tg$^{+/-}$ mice. (**a**) Comparison of protein expression by immunoblot between thymocytes from Themis$^{+/+}$ ΔCore1-Tg$^{+/-}$ and Themis$^{+/+}$ ΔCore2-Tg$^{+/+}$. (**b**) CD4 and CD8 expression profiles of thymocytes from Themis$^{+/+}$ and Themis$^{+/+}$ mice expressing heterozygous ΔCore1-Tg$^{+/-}$ and Themis ΔCore2-Tg$^{+/+}$. Numbers in plots show the frequency of cells in the indicated area. Results are representative of three independent experiments. (**c**) Proportion of post-selected CD69^{+}TCRβ^{hi} DP cells in each mutant. Results are representative of three independent experiments.
(EPS)

Acknowledgments

We would like to thank Masashi Yoshida and Sachiko Nitta for expert technical assistance.

Author Contributions

Conceived and designed the experiments: HS. Performed the experiments: T. Okada TN HO AT MSP KK NT. Analyzed the data: T. Okada TN HS. Contributed reagents/materials/analysis tools: NT MG T. Okamura. Wrote the paper: T. Okada TN HS.

References

1. Rothenberg EV, Taghon T (2005) Molecular genetics of T cell development. Anne Rev Immunol 23: 601–649
2. Patrick MS, Oda H, Hayakawa K, Sato Y, Eshima K, et al. (2009) Gasp, a Grb2-associating protein, is critical for positive selection of thymocytes. Proc Natl Acad Sci USA 106: 16345–16350
3. Lesourne R, Uehara S, Lee J, Song KD, Li L, et al. (2009) Themis, a T cell-specific protein important for late thymocyte development. Nat Immunol 10: 840–847
4. Johnson AL, Aravind L, Shulzhenko N, Morgun A, Choi SY, et al. (2009) Themis is a member of a new metazoan gene family and is required for the completion of thymocyte positive selection. Nat Immunol 10: 831–839
5. Fu G, Vallée S, Rybakin V, McGuire MV, Ampudia J, et al. (2009) Themis controls thymocyte selection through regulation of T cell antigen receptor-mediated signaling. Nat Immunol 10: 848–856
6. Kakugawa K, Yasuda T, Miura I, Kobayashi A, Fukiage H, et al. (2009) A novel gene essential for the development of single positive thymocytes. Mol Cell Biol 29: 5128–5135
7. Marson A, Kretschmer K, Frampton GM, Jacobsen ES, Polansky JK, et al. (2007) Foxp3 occupancy and regulation of key target gens during T-cell stimulation. Nature 445: 931–935
8. Chabod M, Pedros C, Lamouroux L, Colacios C, Bernard I, et al. (2012) A spontaneous mutation of the rat Themis gene leads to impaired function of regulatory T cells linked to inflammatory bowel disease. PLoS Genet 8: e1002461
9. Lesourne R, Zvezdova E, Song KD, EI-Khoury, Uehara S, et al. (2012) Interchangeability of Themis1 and Themis2 in Thymocyte Development Reveals Two Related Proteins with Conserved Molecular Function. J Immunol 189: 1154–1161
10. Brockmeyer C, Paster W, Pepper D, Tan CP, Trudgian DC, et al. (2011) T cell receptor (TCR)- induced tyrosine phosphorylation dynamics identifies THEMIS as a new TCR signalosome component. J Biol Chem 286: 7535–7547
11. Paster W, Brockmeyer C, Fu G, Simister PC, de Wet B, et al. (2013) GRB2-Mediated Recruitment of THEMIS to LAT Is Essential for Thymocyte Development. J Immunol 190: 3749–3756
12. Zhumabekov T, Corbella P, Tolaini M, Kioussis D (1995) Improved version of a human CD2 minigenebased vector for T cell-specific expression in transgenic mice. J Immunol Methods 185: 133–140
13. Pagès G, Guérin S, Grall D, Bonino F, Smith A, et al. (1999) Defective thymocyte maturation in p44 MAP kinase (Erk1) knockout mice. Science 286: 1374–1377
14. Jang IK, Chiang YJ, Kole HK, Cronshaw DG, Zou Y, et al. (2010) Grb2 functions at the top of the T-cell antigen receptor-induced tyrosine kinase cascade to control thymic selection. Proc Natl Acad Sci USA 107: 10620–10625
15. Chardin P, Camonis JH, Gale NW, van Aelst L, Schlessinger J, et al. (1993) Human Sos1: a guanine nucleotide exchange factor for Ras that binds to GRB2. Science 260: 1338–1343
16. Rozakis-Adock M, McGlade J, Mbamalu G, Pelicci G, Daly R, et al. (1992) Association of the Shc and Grb2/Sem5 SH2-containing proteins is implicated in activation of the Ras pathway by tyrosine kinases. Nature 360: 689–692.
17. Schlaepfer DD, Hunter T (1996) Evidence for in vivo phosphorylation of the Grb2 SH2-domain binding site on focal adhesion kinase by Src-familyprotein-tyrosine kinases. Mol Cell Biol 16: 5623–5633
18. Kortum RL, Sommers CL, Pinski JM, Alexander CP, Merrill RK, et al. (2012) Deconstructing Ras signaling in the thymus. Mol Cell Biol 32: 2748–2759.